Supplementary Material (ESI) for Chemical Communications

Electronic supplementary information for:

Allosteric Regulation of Metal-Binding Sites inside an Optically-Active Helical Foldamer and Its Tubular Assemblies

Satoshi Kawabata, Naoki Ousaka[§,]* and Eiji Yashima[§,]*

Department of Molecular Design and Engineering, Graduate School of Engineering, Nagoya University, Chikusa-ku, Nagoya 464-8603, Japan

[§]Present address: Department of Molecular and Macromolecular Chemistry, Graduate School of Engineering, Nagoya University, Nagoya 464-8603, Japan

*To whom correspondence should be addressed.

E-mail: ousaka@chembio.nagoya-u.ac.jp (N.O.); yashima@chembio.nagoya-u.ac.jp (E.Y.)

Table of Contents:

Experimental Section

Instruments

The melting points were measured on a Yanaco MP-500D micromelting point apparatus (Yanako, Kyoto, Japan) and were uncorrected. The IR spectra were recorded on a JASCO FT/IR-680 spectrophotometer (JASCO, Tokyo, Japan). The NMR spectra were measured using a Bruker Ascend 500 (Bruker Biospin, Billerica, MA) or a Varian 500AS (Varian, Palo Alto, CA) spectrometer operating at 500 MHz for ^{1}H and 125 MHz for ^{13}C using tetramethylsilane (TMS) or a solvent residual peak as the internal standard. The absorption and CD spectra were measured in a 0.1-, 0.2-, or 1.0-cm quartz cell on a JASCO V-570 spectrophotometer and a JASCO J-1500 spectropolarimeter, respectively. The temperature was controlled with a JASCO ETC-505 apparatus. The electrospray ionization (ESI) mass spectra were recorded using a JEOL JMS-T100CS mass spectrometer (JEOL, Akishima, Japan). The size exclusion chromatography (SEC) measurements were performed with a JASCO PU-980 liquid chromatograph equipped with an UV-visible detector (324 nm, JASCO UV-2075) and a column oven (JASCO CO-2060). The wide-angle X-ray diffraction (WAXD) measurements were carried out by a Rigaku FR-E/R-AXIS IV system with a rotating-anode generator with graphite monochromated Cu *K*α radiation (l = 0.15418 nm) focused through a 0.3 mm pinhole collimator, which was supplied at 45 kV and 45 mA current, equipped with a flat imaging plate camera having a specimen-to-plate distance of 300 mm. The small-angle X-ray diffraction (SAXD) measurements were carried out by a Rigaku NANO-Viewer X-ray diffractometer using Cu *K*α radiation (l = 0.15418 nm) as an X-ray source and an imaging plate (Fujifilm) for detection. An image was obtained by exposure for 8–22 h. The diameter of the pinhole slit-collimated X-ray beam was in the range of 0.3–0.6 mm. The camera length was set at 955 mm. The number-average molecular weight (M_n) and its distribution (M_w/M_n) were determined at 50 °C using a TSKgel G4000H$_{HR}$ (0.78 (i.d.) × 30 cm) SEC column (Tosoh, Tokyo, Japan), and DMSO/$CHCl_3$ (1/9, v/v) with 0.5 wt% tetra-*n*-butylammonium bromide (TBAB) was used as the eluent at a flow rate of 0.4 mL/min. The molecular weight calibration curve was obtained with polystyrene standards (Tosoh). The atomic force microscopy (AFM) measurements were performed using a Nanoscope V microscope (Bruker AXS, Santa Barbara, CA) in air at room temperature with standard cantilevers (TESP–V2, Bruker AXS) in the tapping mode.

Materials

All starting materials were purchased from commercial suppliers and were used without further purification unless otherwise noted. *N*-(2-Aminoethyl)-3,4,5-tris(dodecyloxy)benzamide (**4**) was prepared according to the literature.[S1]

Synthetic Procedures

Abbreviations of chemicals:

Boc: *tert*-butoxycarbonyl,

dppf: 1,1'-bis(diphenylphosphino)ferrocene,

EDC·HCl: 1-ethyl-3-(3-dimethylaminopropyl)-carbodiimide hydrochloride,

HOBt·H_2O: 1-hydroxybenzotriazole monohydrate,

$^{i}Pr_2NH$: diisopropylamine,

NMM: *N*-methylmorphiline,

TFA: trifluoroacetic acid.

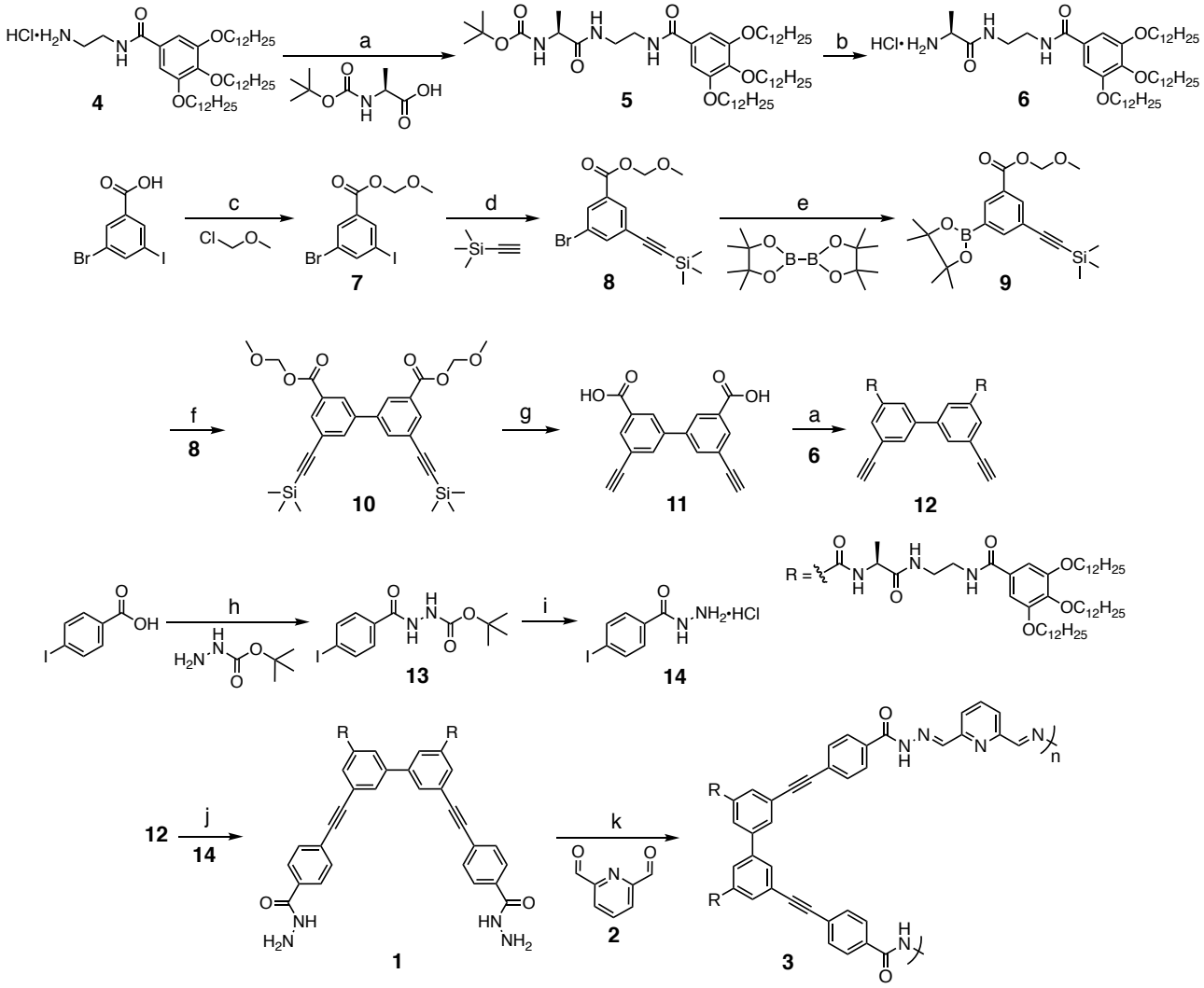

Scheme S1. Synthesis of **3**. Reagents and conditions: a) HOBt·H_2O, EDC·HCl, NMM, DMF, 0 °C to r.t. b) 4N HCl in 1,4-dioxane, 0 ºC. c) Et_3N, THF, 0 °C to r.t. d) $Pd(PPh_3)_2Cl_2$, PPh_3, CuI, Et_3N, THF, 0 °C to r.t. e) $Pd(dppf)Cl_2·CH_2Cl_2$, KOAc, 1,4-dioxane, 80 °C. f) K_3PO_4, $Pd(PPh_3)_4$, 1,4-dioxane, 110 ºC. g) aqueous NaOH, MeOH, THF, r.t. h) EDC·HCl, CH_2Cl_2, 0°C to r.t. i) 4N HCl in 1,4-dioxane, 0 ºC to r.t. j) $Pd(PPh_3)_4$, CuI, $^{i}Pr_2NH$, THF, 40 °C. k) TFA, THF, DMSO, 50 °C.

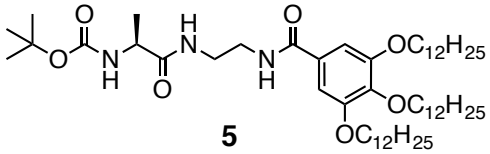

5

5. To a solution of **4** (1.00 g, 1.33 mmol), Boc-L-alanine (278 mg, 1.47 mmol), and HOBt·H_2O (265 mg, 1.73 mmol) in DMF (20 mL) was added EDC·HCl (258 mg, 1.34 mmol) at 0 ºC under N_2, and the reaction mixture was stirred at 0 °C for 1 h. After NMM (0.151 mL, 1.37 mmol) was added to this at 0 ºC, the reaction mixture was stirred at 0 ºC for 30 min and further at room temperature for 11.5 h. After evaporating the solvent under reduced pressure, the residue was dissolved in $CHCl_3$, and the solution was washed with 1N aqueous HCl, 5% aqueous $NaHCO_3$, and brine, dried over $MgSO_4$, filtered, and evaporated to dryness under reduced pressure, affording **5** (1.05 g, 89.3%) as a white solid. Mp: 85–87 °C. ^{1}H NMR (500 MHz, $CDCl_3$, 25 °C): δ 7.18 (br, 1H, NH), 7.04 (s, 2H, Ar-H), 6.88 (br, 1H, NH), 5.00 (br, 1H, NH), 4.13 (br, 1H, NCHCO), 4.02-3.97 (m, 6H, OCH_2), 3.58-3.49 (m, 4H, NCH_2), 1.82-1.72 (m, 6H, CH_2), 1.46-1.26 (m, 66H, CH_2, CH_3), 0.89-0.87 (m, 9H, CH_3). ^{13}C NMR (125 MHz, $CDCl_3$, 25 °C): δ 174.36, 167.89, 155.60, 153.04, 141.01, 128.82, 105.61, 80.38, 73.47, 69.20, 50.46, 41.13, 39.68, 31.94, 30.34, 29.77, 29.75, 29.73, 29.676, 29.61, 29.44, 29.40, 29.38, 28.28, 26.13, 26.10, 22.71, 18.19, 14.13. IR (KBr, cm^{-1}): 3289 (ν_{N-H}), 1688 ($\nu_{C=O}$), 1659 ($\nu_{C=O}$), 1582 (ν_{N-H}), 1539 (ν_{N-H}). HRMS (ESI-MS): *m*/*z* calcd for [M($C_{53}H_{97}N_3O$) + H]$^+$, 888.7405; found 888.7398.

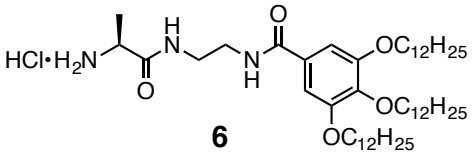

6

6. Into a two-neck round bottom flask containing **5** (993 mg, 1.12 mmol) was added 4N HCl in 1,4-dioxane (20 mL) at 0 ºC under N_2, and the reaction mixture was stirred at 0 ºC for 5 h. After evaporating the solvent under reduced pressure, the residue was washed with Et_2O to afford **6** (902 mg, 98%) as a white solid. Mp: 210–212 °C. ^{1}H NMR (500 MHz, DMSO-d_6/$CDCl_3$ (1/9, v/v), 25 °C): δ 8.82 (br, 1H, NH), 8.61 (br, 1H, NH), 8.44 (s, 3H, NH_3^+), 7.34 (s, 2H, Ar-H), 4.10-3.95 (m, 7H, OCH_2, N-CH-CO), 3.63-3.33 (m, 4H, N-CH_2), 1.82-1.70 (m, 6H, CH_2), 1.51-1.47 (m, 9H, CH_2, CH_3), 1.30-1.26 (m, 48H, CH_2), 0.88 (m, 9H, CH_2). ^{13}C NMR (125 MHz, DMSO-d_6/$CDCl_3$ (1/9, v/v), 25 °C): δ 169.64, 167.14, 152.72, 140.33, 129.04, 106.08, 73.26, 69.16, 49.68, 40.60, 40.44, 40.27, 40.10, 39.93, 39.77, 39.60, 38.98, 31.85, 31.84, 30.28, 29.67, 29.65, 29.63, 29.59, 29.58, 29.53, 29.41, 29.37, 29.30, 29.28, 26.113, 26.04, 22.60, 17.00, 14.10. IR (KBr, cm^{-1}): 3266

(ν_{N-H}), 1681 ($\nu_{C=O}$), 1634 ($\nu_{C=O}$), 1582 (ν_{N-H}), 1549 (ν_{N-H}). HRMS (ESI-MS): *m*/*z* calcd for $[M(C_{48}H_{89}N_3O_5) + H]^+$, 788.6880; found 788.6889.

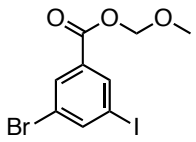

7

7. To a solution of 3-bromo-5-iodobenzoic acid (9.96 g, 30.5 mmol) in THF (80 mL) were added Et_3N (5.0 mL) and chloromethyl methyl ether (2.80 mL, 37.0 mmol) at 0 °C under Ar, and the reaction mixture was stirred at 0 °C for 1 h and further at room temperature for 12 h. After evaporating the solvent under reduced pressure, the residue was dissolved in EtOAc, and the solution was washed with 5% aqueous $NaHCO_3$ and brine, dried over $MgSO_4$, filtered, and concentrated under reduced pressure. The crude product was purified by column chromatography (SiO_2, *n*-hexane/EtOAc (1/1, v/v)) to afford **7** (11.0 g, 98%) as a white solid. Mp: 72-73 °C. ^{1}H NMR (500 MHz, $CDCl_3$, 25 °C): δ 8.32 (dd, J =1.5, 1.5 Hz, 1H, Ar-H), 8.16 (dd, J =1.5, 1.7 Hz, 1H, Ar-H), 8.06 (dd, J =1.8, 1.7 Hz, 1H, Ar-H), 5.48 (s, 2H, CH_2), 3.56 (s, 3H, OCH_3). ^{13}C NMR (125 MHz, $CDCl_3$, 25 °C): δ 163.51, 144.24, 137.42, 133.16, 132.23, 123.23, 94.22, 91.83, 58.20. IR (KBr, cm^{-1}): 1727 ($\nu_{C=O}$). Anal. Calcd for $C_9H_8BrIO_3$: C, 29.14; H, 2.17; Found: C, 29.14; H, 2.10.

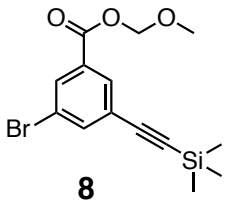

8

8. Into a two-neck round bottom flask containing **7** (7.00g, 18.9 mmol), $Pd(PPh_3)_2Cl_2$ (265 mg, 0.377 mmol), PPh_3 (98.9 mg, 0.377 mmol), and CuI (71.8 mg, 0.377 mmol) were added THF (100 mL) and Et_3N (70 mL) under Ar. After dissolving, the flask was cooled to −78 °C (dry ice-methanol), and subjected to three evacuation/Ar fill cycles. The flask was then warmed to 0 °C, trimethylsilyl acetylene (2.80 mL, 19.8 mmol) was added to this under Ar with stirring. The reaction mixture was stirred at 0 °C for 1 h and further at room temperature for 12 h. After evaporating the solvent under reduced pressure, the residue was dissolved in EtOAc, and the solution was washed with 1N aqueous HCl and brine, dried over $MgSO_4$, filtered, and concentrated under reduced pressure. The crude product was purified by column chromatography (SiO_2,

n-hexane/EtOAc (9/1, v/v)) to afford **8** (5.94 g, 92%) as a white solid. Mp: 79-80 °C. ^{1}H NMR (500 MHz, $CDCl_3$, 25 °C): δ 8.13 (dd, J = 2.0, 1.5 Hz, 1H, Ar-H), 8.07 (dd, J =1.5, 1.5 Hz, 1H, Ar-H), 7.80 (dd, J =1.5, 1.5 Hz, 1H, Ar-H), 5.48 (s, 2H, CH_2), 3.56 (s, 3H, OCH_3), 0.26 (s, 9H, $Si(CH_3)_3$). ^{13}C NMR (125 MHz, $CDCl_3$, 25 °C): δ 164.25, 139.03, 132.67, 131.88, 131.81, 125.67, 122.32, 102.24, 97.50, 91.68, 58.13, -0.11. IR (KBr, cm^{-1}): 2158 ($\nu_{C\equiv C}$), 1729 ($\nu_{C=O}$). Anal. Calcd for $C_{14}H_{17}BrO_3Si$: C, 49.27; H, 5.02. Found: C, 49.28; H, 5.01.

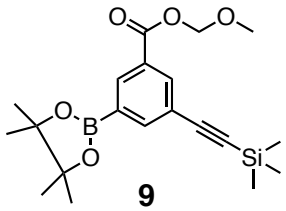

9

9. Into a two-neck round bottom flask containing **8** (5.92 g, 17.3 mmol), bis(pinacolato)diboron (4.68 g, 18.4 mmol), $Pd(dppf)Cl_2 \cdot CH_2Cl_2$ (1.25 g, 1.53 mmol), and KOAc (5.11 g, 52.0 mmol) was added 1,4-dioxane (110 mL) under Ar. After dissolving, the flask was subjected to five evacuation/Ar fill cycles, and the reaction mixture was stirred at 80 °C for 16 h. After evaporating the solvent under reduced pressure, the residue was dissolved in EtOAc, and the solution was washed with H_2O and brine, dried over $MgSO_4$, filtered, and concentrated under reduced pressure. The crude product was purified by column chromatography (SiO_2, *n*-hexane/EtOAc (9/1, v/v)) to afford **9** (5.93 g, 88%) as a colorless oil. ^{1}H NMR (500 MHz, $CDCl_3$, 25 °C): δ 8.42 (dd, J = 1.7, 1.2 Hz, 1H, Ar-H), 8.24 (dd, J = 1.8, 1.8 Hz, 1H, Ar-H), 8.11 (dd, J = 1.6, 1.2 Hz, 1H, Ar-H), 5.49 (s, 2H, OCH_2), 3.55 (s, 3H, OCH_3), 1.35 (s, 12H, $C(CH_3)_2$), 0.25 (s, 9H, $Si(CH_3)_3$). ^{13}C NMR (125 MHz, $CDCl_3$, 25 °C): δ 165.59, 142.88, 135.75, 135.67, 129.61, 123.43, 103.90, 95.59, 91.23, 84.48, 58.03, 58.01, 25.00, 0.02. IR (KBr, cm^{-1}): 2159 ($\nu_{C\equiv C}$), 1733 ($\nu_{C=O}$). HRMS (ESI-MS): m/z calcd for $[M(C_{20}H_{29}BO_5Si) + Na]^+$, 411.1779; found 411.1792.

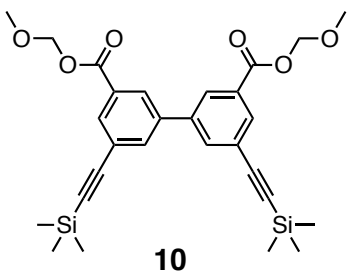

10

10. Into a two-neck round bottom flask containing **8** (1.94 g, 5.69 mmol), **9** (2.00 g, 5.14 mmol), K_3PO_4 (2.22 g, 10.4 mmol), and $Pd(PPh_3)_4$ (597 mg, 516 mmol) was added 1,4-dioxane (60 mL)

under Ar. The flask was then subjected to three evacuation/Ar fill cycles, and the reaction mixture was stirred at 110 °C for 16 h. After cooling to room temperature, the solvent was evaporated to dryness under reduced pressure. The residue was dissolved in EtOAc, and the solution was washed with H_2O and brine, dried over $MgSO_4$, filtered, and concentrated under reduced pressure. The crude product was purified by column chromatography (SiO_2, *n*-hexane/EtOAc (4/1, v/v)) to afford **10** (1.58 g, 59%) as a colorless oil. ^{1}H NMR (500 MHz, $CDCl_3$, 25 °C): δ 8.25 (dd, J = 1.5, 1.5 Hz, 2H, Ar-H), 8.19 (dd, J = 1.5, 1.5 Hz, 2H, Ar-H), 7.92 (dd, J = 1.5, 1.5 Hz, 2H, Ar-H), 5.53 (s, 4H, OCH_2), 3.59 (s, 6H, OCH_3), 0.29 (s, 18H, $Si(CH_3)_3$). ^{13}C NMR (125 MHz, $CDCl_3$, 25 °C): δ 165.26, 139.97, 135.03, 132.71, 131.01, 128.33, 124.69, 103.46, 96.47, 91.52, 58.12, -0.0184. IR (KBr, cm^{-1}): 2158 ($\nu_{C\equiv C}$), 1730 ($\nu_{C=O}$). HRMS (ESI-MS): *m*/*z* calcd for $[M(C_{28}H_{34}O_6Si_2) + Na]^+$, 545.1792; found 545.1790.

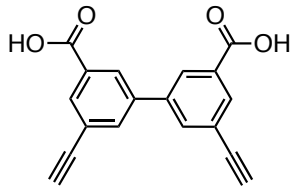

11

11. To a solution of **10** (1.28 g, 2.46 mmol) in MeOH (8.0 mL) and THF (16.0 mL) was added 1N aqueous NaOH (16.0 mL, 16.0 mmol) at 0 °C under N_2, and the reaction mixture was stirred at 0 °C for 5 min and further at room temperature for 3 h. After most of the organic solvents was removed under reduced pressure, the solution was washed with Et_2O and then acidified to pH 1–2 by 1N aqueous HCl. The precipitate was collected by filtration, washed with water and *n*-hexane, and dried in vacuo, affording **11** (717 mg, quant.) as a white sold. Mp: 219 °C (dec.). ^{1}H NMR (500 MHz, DMSO-d_6, 25 °C): δ 13.41 (s, 2H, COOH), 8.19 (dd, J = 1.6, 1.6 Hz, 2H, Ar-H), 8.10 (dd, J = 1.6, 1.6 Hz, 2H, Ar-H), 8.00 (dd, J = 1.6, 1.6 Hz, 2H, Ar-H), 4.39 (s, 2H, C≡CH). ^{13}C NMR (125 MHz, DMSO-d_6, 25 °C): δ 166.21, 139.28, 134.10, 132.25, 131.80, 127.95, 123.11, 82.22. IR (KBr, cm^{-1}): 3290 ($\nu_{\equiv C-H}$), 2975 (ν_{O-H}). HRMS (ESI-MS): *m*/*z* calcd for $[M(C_{18}H_{10}O_4) - H]^-$, 289.0501; found 289.0492.

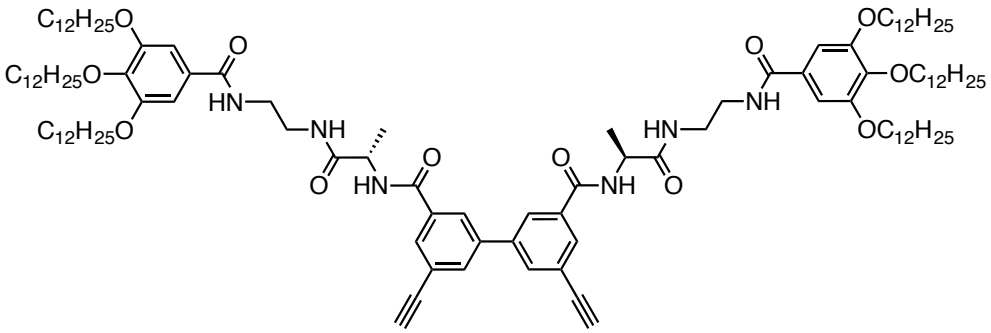

12

12. To a solution of **11** (148 mg, 0.509 mmol), **6** (879 mg, 1.07 mmol), and HOBt·H_2O (195 mg, 1.28 mmol) in DMF (15 mL) was added EDC·HCl (198 mg, 1.03 mmol) at 0 ºC under N_2, and the reaction mixture was stirred at 0 °C for 1 h. After NMM (0.125mL, 1.14 mmol) was added to this at 0 ºC, the reaction mixture was stirred at 0 ºC for 30 min and further at room temperature for 25 h. After evaporating the solvent under reduced pressure, the residue was dissolved in $CHCl_3$, and the solution was washed with 1N aqueous HCl, 5% aqueous $NaHCO_3$, and brine, dried over $MgSO_4$, filtered, and concentrated under reduced pressure. The crude product was purified by column chromatography (SiO_2, MeOH/$CHCl_3$ (1/9, v/v)) to afford **12** (616 mg, 66%) as a slightly yellowish solid. Mp: 201–203 °C. ^{1}H NMR (500 MHz, DMSO-d_6/$CDCl_3$ (1/9, v/v), 50 °C): δ 8.47 (s, 2H, NH), 8.17 (s, 2H, Ar-H), 7.98 (s, 2H, Ar-H), 7.82 (s, 2H, NH), 7.76 (s, 2H, Ar-H), 7.71 (s, 2H, NH), 7.05 (s, 4H, Ar-H), 4.73 (m, 2H, NCHCO), 3.96-3.89 (s, 6H, OCH_2), 3.51 (m, 4H, NCH_2), 3.40 (m, 4H, NCH_2), 3.19 (s, 2H, C≡CH), 1.77-1.68 (m, 12H, CH_2), 1.49-1.40 (m, 18H, CH_2, CH_3), 1.26 (m, 96H, CH_2), 0.88 (m, 18H, CH_3). ^{13}C NMR (125 MHz, DMSO-d_6/$CDCl_3$ (1/9, v/v), 50 °C): δ 173.68, 167.63, 165.60, 152.61, 140.87, 139.66, 134.66132.95, 130.69, 128.96, 126.03, 122.93, 106.04, 82.33, 78.45, 73.11, 69.03, 49.77, 31.59, 31.58, 30.08, 29.40, 29.38, 29.36, 29.33, 29.31, 29.27, 29.18, 29.12, 29.01, 29.00, 25.85, 25.81, 22.32, 17.76, 13.74. IR (KBr, cm^{-1}): 3265 ($\nu_{\equiv C-H}$), 1634 ($\nu_{C=O}$), 1538 (ν_{N-H}). HRMS (ESI-MS): *m*/*z* calcd for $[M(C_{114}H_{184}N_6O_{12}) + Na]^+$, 1852.3870; found 1852.3797.

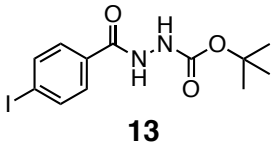

13

13. To a solution of 4-iodobenzoic acid (5.37 g, 21.6 mmol) in CH_2Cl_2 (200 mL) was added EDC·HCl (5.06 g, 26.4 mmol) at 0 ºC under N_2 and the reaction mixture was stirred at 0 °C for 30 min. After *tert*-butyl carbazate (3.00 g, 22.7 mmol) was added to this at 0 ºC, the reaction mixture

was stirred at 0 ºC for 30 min and further at room temperature for 84 h. The solution was diluted with CH_2Cl_2, and the solution was washed with 5% aqueous $NaHCO_3$ and brine, dried over Na_2SO_4, filtered, and evaporated to dryness under reduced pressure. The crude product was purified by column chromatography (SiO_2, $CHCl_3$/*n*-hexane/EtOAc (1/1/2, v/v/v)) to afford **13** (5.87 g, 75%) as a white solid. Mp: 166–167 °C. ^{1}H NMR (500 MHz, $CDCl_3$, 25 °C): δ 8.79 (br, 1H, NH), 7.72 (d, J = 8.3 Hz, 2H, Ar-H), 7.49 (d, J = 8.3 Hz, 2H, Ar-H), 6.83 (br, 1H, NH), 1.48 (s, 9H, CH_3). ^{13}C NMR (125 MHz, $CDCl_3$, 25 °C): δ 166.21, 156.21, 137.93, 131.05, 128.90, 99.70, 82.43, 28.28. IR (KBr, cm^{-1}): 3339 (ν_{N-H}), 3230 (ν_{N-H}), 1720 ($\nu_{C=O}$), 1664 ($\nu_{C=O}$). HRMS (ESI-MS): *m*/*z* calcd for $[M(C_{12}H_{15}N_2O_3I) - H]^-$, 361.0049; found 361.0060.

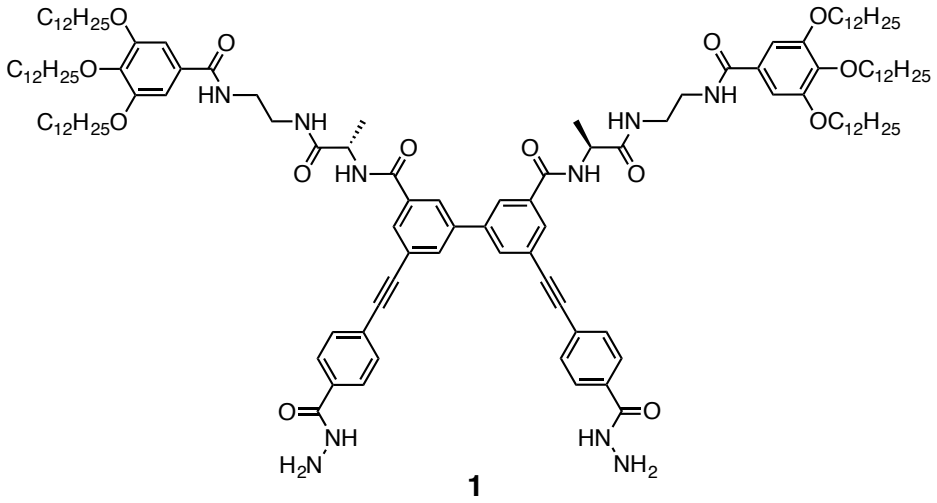

1

1. 13 was dissolved in 4N HCl in 1,4-dioxane at 0 °C. The reaction mixture was stirred at room temperature for 4 h and the solvent was evaporated to dryness under reduced pressure, affording **14** as a white solid, which was used without further purification in the next step. Into a two-neck round bottom flask containing **12** (251 mg, 0.137 mmol) and **14** (205 mg, 0.687 mmol) was added dry THF (10 mL) under Ar. After dissolving, the solution was frozen by liq. N_2 and degassed by three freeze-pump-thaw cycles. After the flask was warmed to 0 °C, to this were added $Pd(PPh_3)_4$ (5.11 mg, 7.28 μmol), CuI (1.39 mg, 7.30 μmol), and degassed ^{i}Pr$_2$NH (2.5 mL) under Ar, and the solution was gradually warmed to room temperature. The reaction mixture was stirred at room temperature for 20 min and further at 40 °C for 17 h. After cooling to room temperature, to this was added excess MeOH (100 mL) and the precipitate was collected by filtration and washed with MeOH, affording **1** (253 mg, 88%) as a brown solid. Mp: 270 °C (dec.). ^{1}H NMR (500 MHz, DMSO-d_6/$CDCl_3$ (3/7, v/v), 25 °C): δ 9.81 (br, 2H, NH), 8.66 (br, 2H, NH), 8.34 (s, 2H, Ar-H), 8.22 (br, 2H, NH), 8.13 (s, 2H, Ar-H), 8.03 (br, 2H, NH), 8.00 (s, 2H, Ar-H), 7.90 (d, J = 7.5 Hz, 4H, Ar-H), 7.58 (d, J = 7.5 Hz, 4H, Ar-H), 7.10 (s, 4H, Ar-H), 4.66 (m, 2H, NCHCO), 4.38 (br, 4H,

NH_2), 3.94-3.89 (m, 12H, OCH_2), 3.52-3.46 (m, 4H, NCH_2), 3.42-3.41 (m, 4H, NCH_2), 1.77-1.65 (m, 12H, CH_2), 1.47 (d, J = 7.0 Hz, 6H, CH_3), 1.44-1.41 (m, 12H, CH_2), 1.28-1.24 (m, 96H, CH_2), 0.88-0.85 (m, 18H, CH_3). ^{13}C NMR (125 MHz, DMSO-d_6/$CDCl_3$ (3/7, v/v), 25 °C): δ 172.85, 166.76, 165.25, 152.04, 139.70, 139.11, 134.86, 131.89, 130.85, 129.97, 128.77, 126.96, 125.99, 124.86, 122.96, 105.27, 89.99, 89.27, 77.96, 72.54, 68.29, 49.25, 38.84, 31.22, 31.21, 29.68, 29.05, 29.04, 29.02, 29.00, 28.97, 28.96, 28.95, 28.930, 28.89, 28.74, 28.66, 28.64, 25.50, 25.43, 21.99, 21.98, 17.51, 13.59. IR (KBr, cm^{-1}): 3310 (ν_{N-H}), 1637 ($\nu_{C=O}$), 1541 (ν_{N-H}). HRMS (ESI-MS): m/z calcd for $[M(C_{128}H_{196}N_{10}O_{14}) + Na]^+$, 2120.4830; found 2120.4793.

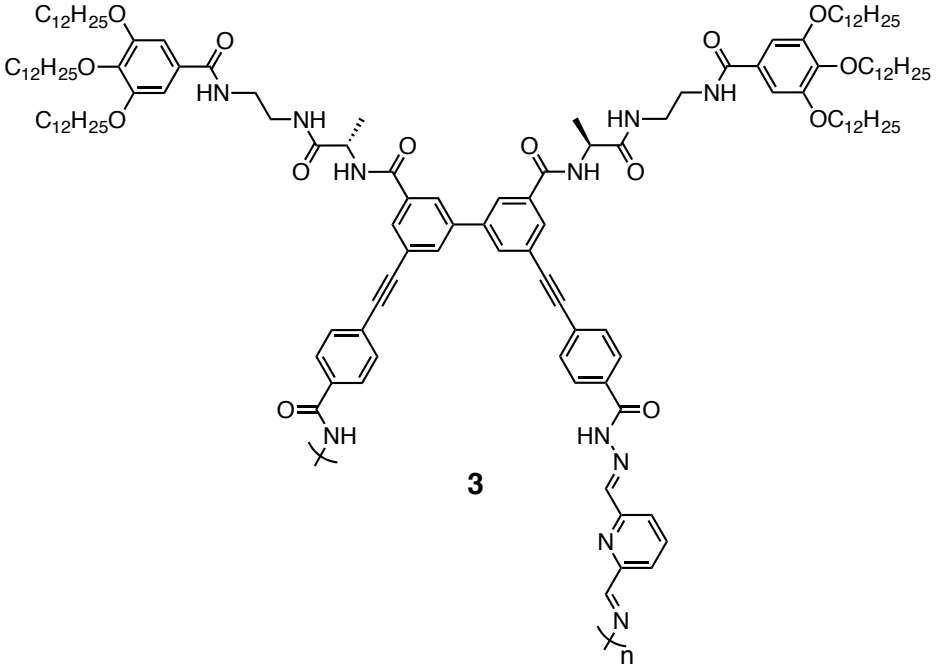

3

3. Into a two-neck round bottom flask containing **1** (72.7 mg, 34.6 μmol) was added **2** (4.70 mg, 34.8 μmol) in DMSO (0.6 mL) and THF (1.5 mL), and the reaction mixture was stirred at 50 °C for 30 min. After a catalytic amount of TFA (3.5 μmol) in DMSO (60 μL) and THF (140 μL) was added to this, the reaction mixture was stirred at 50 °C for 3 days. To this was then added excess MeOH (20 mL) and the precipitate was collected and washed with MeOH. The crude product was purified by SEC (TOYOPEARL HW-50S (1.5 (i.d.) × 88 cm), DMF/THF (3/7, v/v)), affording **3** (25.9 mg, 34%) as a yellow solid. The M_n and M_w/M_n of **3** were estimated to be 1.7×10^4 and 1.2, respectively, by SEC with polystyrene standard using DMSO/$CHCl_3$ (1/9, v/v) with 0.5 wt% TBAB as the eluent at a flow rate of 0.4 mL/min.

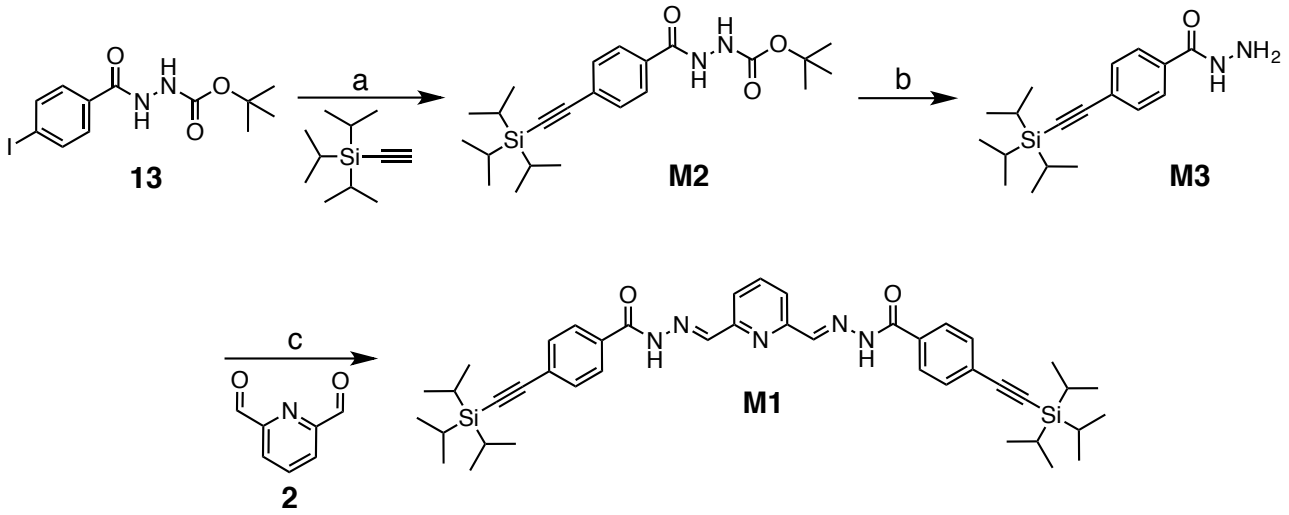

Scheme S2. Synthesis of **M1**. Reagents and conditions: a) $Pd(PPh_3)_2Cl_2$, PPh_3, CuI, Et_3N, THF, 40 ºC. b) 4N HCl in 1,4-dioxane, 0°C to r.t. c) THF, 40 °C.

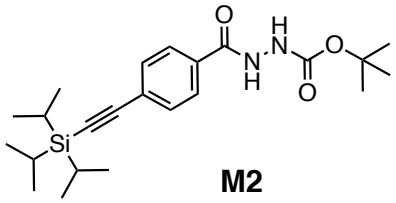

M2. Into a two-neck round bottom flask containing **13** (700 mg, 1.93 mmol), $Pd(PPh_3)_2Cl_2$ (68.2 mg, 97.1 μmol), PPh_3 (28.1 mg, 0.107 mmol), and CuI (19.2 mg, 0.101 mmol) were added THF (2.0 mL) and Et_3N (5.4 mL) under N_2. After dissolving, the flask was cooled to −78 °C (dry ice-methanol), and subjected to three evacuation/N_2 fill cycles. After the flask was warmed to 0 °C, to this was added triisopropylsilyl acetylene (0.57 mL, 2.5 mmol). The reaction mixture was stirred at 0 °C for 10 min and further at 40 °C for 15 h. After evaporating the solvent under reduced pressure, the residue was dissolved in EtOAc, and the solution was washed with H_2O and brine, dried over Na_2SO_4, filtered, and concentrated under reduced pressure. The crude product was purified by column chromatography (SiO_2, $CHCl_3$/EtOAc (9/1, v/v)) to afford **M2** (655 mg, 81%) as a white solid. Mp: 193–194 °C. ^{1}H NMR (500 MHz, $CDCl_3$, 25 °C): δ 8.75 (br, 1H, NH), 7.72 (d, J = 8.3 Hz, 2H, Ar-H), 7.46 (d, J = 8.3 Hz, 2H, Ar-H), 6.88 (br, 1H, NH), 1.45 (s, 9H, CH_3), 1.16-1.10 (m, 21H, CH, CH_3). ^{13}C NMR (125 MHz, $CDCl_3$, 25 °C): δ 166.25, 156.14, 132.25, 131.05, 127.64, 127.28, 106.09, 94.15, 82.297, 28.27, 18.78, 11.40. IR (KBr, cm^{-1}): 3335 ($\nu_{N\text{-}H}$), 3220 ($\nu_{N\text{-}H}$), 2156 ($\nu_{C\equiv C}$), 1721 ($\nu_{C=O}$), 1659 ($\nu_{C=O}$). HRMS (ESI-MS): m/z calcd for $[M(C_{23}H_{36}N_2O_3Si) + Na]^+$, 439.2393; found 439.2399.

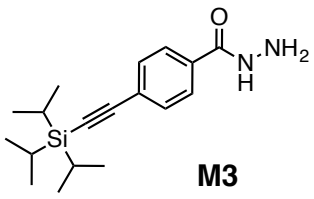

M3

M3. M2 (512 mg, 1.23 mmol) was dissolved in 4N HCl in 1,4-dioxane at 0 ºC under N_2, and the reaction mixture was stirred at 0 ºC for 1 h and further at room temperature for 2 h. After evaporating the solvent under reduced pressure, the residue was dissolved in EtOAc, and the solution was washed with 5% aqueous $NaHCO_3$ and brine, dried over Na_2SO_4, filtered, and evaporated to dryness under reduced pressure. The residue was washed with *n*-hexane to afford **M3** (349 mg, 89%) as a white solid. Mp: 118–119 °C. ^{1}H NMR (500 MHz, $CDCl_3$, 25 °C): δ 7.87 (br, 1H, NH), 7.71 (d, J = 8.3 Hz, 2H, Ar-H), 7.53 (d, J = 8.3 Hz, 2H, Ar-H), 4.16 (br, 2H, NH_2), 1.16-1.10 (m, 21H, CH, CH_3). ^{13}C NMR (125 MHz, $CDCl_3$, 25 °C): δ 168.10, 132.37, 132.03, 127.36, 126.89, 106.02, 94.09, 18.76, 11.38. IR (KBr, cm^{-1}): 3314 (ν_{N-H}), 2155 ($\nu_{C\equiv C}$), 1667 ($\nu_{C=O}$). HRMS (ESI-MS): *m*/*z* calcd for [M($C_{23}H_{36}N_2O_3Si$) + Na]$^+$, 339.1869; found 339.1875.

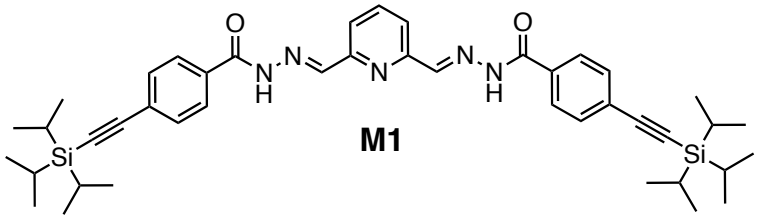

M1

M1. M3 (253 mg, 799 mmol) and **2** (51.2 mg, 379 mmol) were dissolved in THF (2.5 mL) under N_2, and the reaction mixture was stirred at room temperature for 1 h and further at 40 °C for 7 h. After evaporating the solvent under reduced pressure, the residue was washed with Et_2O to afford **M1** (244 mg, 88%) as a white solid. Mp: 271–272 °C. ^{1}H NMR (500 MHz, DMSO-d_6, 25 °C): δ 12.16 (br, 2H, NH), 8.53 (s, 2H, N=CH), 8.01 (br, 3H, Py-H), 7.97 (d, J = 8.0 Hz, 4H, Ar-H), 7.64 (d, J = 8.0 Hz, 4H, Ar-H), 1.16-1.10 (m, 42H, CH, CH_3). ^{13}C NMR (125 MHz, DMSO-d_6, 25 °C): δ 162.42, 153.23, 147.81, 137.76, 132.93, 131.86, 128.10, 125.73, 120.57, 106.31, 92.97, 18.50, 10.69. IR (KBr, cm^{-1}): 3447 (ν_{N-H}), 2156 ($\nu_{C\equiv C}$), 1655 ($\nu_{C=O}$). HRMS (ESI-MS): *m*/*z* calcd for [M($C_{43}H_{57}N_5O_2Si_2$) + Na]$^+$, 754.3948; found 754.3923.

Atomic Force Microscopy (AFM) Measurements

AFM Measurements of Assemblies of 1 on Mica

A solution of **1** in $CHCl_3$ (10 μM) was prepared. Samples for the AFM measurements of **1** were prepared by casting 30 μL aliquots of the stock solution on a freshly cleaved mica at room temperature (ca. 25 °C), and the solvents were then slowly evaporated under a $CHCl_3$ vapor atmosphere. After **1** had been deposited on the mica, the mica substrates were exposed to $CHCl_3$ vapors at room temperature for 12 h, and the substrates were then dried under vacuum for 1 h. The organic solvent vapors were prepared by putting 1 mL of $CHCl_3$ into a 2 mL flask that was inside a 50 mL flask, and the mica substrates were then placed in the 50 mL flask. The AFM measurements were performed using a Nanoscope V microscope in air at room temperature with standard silicon cantilevers (TESP–V2) in the tapping mode. The typical settings of the AFM for the high-magnification observations were as follows: a free amplitude of the oscillation frequency of 280 mV, a set-point amplitude of 180–250 mV, and a scan rate of 1.0 Hz. The Nanoscope image processing software was used for the image analysis.

AFM Measurements of 2D Assemblies of 3 on Mica

A solution of **3** in a DMSO/$CHCl_3$ mixture (1/9, v/v, 0.1 mM) was prepared and 5-fold diluted with $CHCl_3$ ([**3**] = 20 μM, DMSO/$CHCl_3$ (*ca.* 2/98, v/v)). Samples for the AFM measurements of **3** were prepared by casting 30 μL aliquots of the stock solution on a freshly cleaved mica at room temperature (ca. 25 °C), and the solvents were then slowly evaporated under a $CHCl_3$ vapor atmosphere. After **3** had been deposited on the mica, the mica substrates were exposed to $CHCl_3$ vapors at room temperature for 13 h, and the substrates were then dried under vacuum for 1 h. The organic solvent vapors were prepared by putting 1 mL of $CHCl_3$ into a 2 mL flask that was inside a 50 mL flask, and the mica substrates were then placed in the 50 mL flask. The AFM measurements were performed using a Nanoscope V microscope in air at room temperature with standard silicon cantilevers (TEPS–V2) in the tapping mode. The typical settings of the AFM for the high-magnification observations were as follows: a free amplitude of the oscillation frequency of 280 mV, a set-point amplitude of 200–250 mV, and a scan rate of 1.0 Hz. The Nanoscope image processing software was used for the image analysis.

AFM Measurements of 2D Assemblies of 3 with $AgBF_4$ on Mica

A solution of **3** in the presence of $AgBF_4$ (1 equiv.) in a DMSO/$CHCl_3$ mixture (1/9, v/v, 0.1 mM) was prepared and 10-fold diluted with $CHCl_3$ ([**3**] = 10 μM, DMSO/$CHCl_3$ (*ca.* 1/99, v/v)). Samples for the AFM measurements of **3** were prepared by casting 30 μL aliquots of the stock

solution on a freshly cleaved mica at room temperature (ca. 25 °C), and the solvents were then slowly evaporated under a $CHCl_3$ vapor atmosphere. After **3** had been deposited on the mica, the mica substrates were exposed to $CHCl_3$ vapors at room temperature for 12 h, and the substrates were then dried under vacuum for 1 h. The organic solvent vapors were prepared by putting 1 mL of $CHCl_3$ into a 2 mL flask that was inside a 50 mL flask, and the mica substrates were then placed in the 50 mL flask. The AFM measurements were performed using a Nanoscope V microscope in air at room temperature with standard silicon cantilevers (TEPS–V2) in the tapping mode. The typical settings of the AFM for the high-magnification observations were as follows: a free amplitude of the oscillation frequency of 280 mV, a set-point amplitude of 200–250 mV, and a scan rate of 1.0 Hz. The Nanoscope image processing software was used for the image analysis.

Molecular Modeling of the Stacked Assemblies of 1, $\mathbf{3}_{(n=8)}$ and $\mathbf{3}_{(n=8)}$ Complexed with Ag(I) Ions ($\mathbf{3}_{(n=8)}$·Ag(I)) to Form $(\mathbf{1})_5$, $(\mathbf{3}_{(n=8)})_4$ and ($\mathbf{3}_{(n=8)}$·Ag(I))$_4$.

The molecular modeling was performed on a Windows 7 or 10 PC with the ArgusLab software[S2] or the MS modeling software (version 8.0, BIOVIA, San Diego, CA).

$(\mathbf{1})_5$. The initial structure of **1** was constructed according to the following procedures: the chiral oligoamide side chains of **1** were replaced with $–CONHCH_3$ groups to simplify the calculations. Based on the CD spectral pattern of the assembled **1** (Figs. 2a and S4), the twist angle between the two phenyl rings of the biphenylene moiety was set to be –45°.[S3] The monomer **1** was then allowed to manually construct a pentamer $(\mathbf{1})_5$ so as to stack each other via intermolecular hydrogen-bonding interactions. The initial model of the stacked $(\mathbf{1})_5$ was fully optimized by the semi-empirical molecular orbital (MO) calculations (PM6 method[S4] in MOPAC2012[S5]) (Fig. 2e).

$(\mathbf{3}_{(n=8)})_4$. The initial structure of $\mathbf{3}_{(n=8)}$ (8 repeating monomer units) was constructed according to the following procedures: tris(dodecyloxy)benzene groups of the chiral oligoamide side chains of $\mathbf{3}_{(n=8)}$ were replaced with tris(methoxy)benzene groups to simplify the calculations. The twist angle between the two phenyl rings of the biphenylene moiety was set to be –45°.[S3] The 2,6-pyridinebis(acylhydrazone) linker units were constructed in such a way to form a planar, extended W-shaped conformation based on the related crystal structure.[S6] The initial model of $\mathbf{3}_{(n=8)}$ was fully optimized by the molecular mechanics (MM) calculations (Compass II force field[S7] as implemented in the MS modeling software) (Fig. S9f, left). In order to estimate the molecular diameter of the self-assembled nanofiber of $\mathbf{3}_{(n=8)}$, helically-stacked tetrameric $\mathbf{3}_{(n=8)}$ ($(\mathbf{3}_{(n=8)})_4$) was constructed according to the following procedures: the energy-minimized $\mathbf{3}_{(n=8)}$ was allowed to manually construct a tetramer $(\mathbf{3}_{(n=8)})_4$ with a twisting angle of –30º between the adjacent $\mathbf{3}_{(n=8)}$ foldamers so as to helically stack each other. The initial model of $(\mathbf{3}_{(n=8)})_4$ was fully optimized by

the MM calculations (Compass II force field) (Fig. S9f, right).

$(\mathbf{3}_{(n=8)}\cdot\mathbf{Ag(I)})_4$. The initial structure of Ag(I)-bound $\mathbf{3}_{(n=8)}$ ($\mathbf{3}_{(n=8)}\cdot$Ag(I)) was constructed according to the following procedures: tris(dodecyloxy)benzene groups of the chiral oligoamide side chains of $\mathbf{3}_{(n=8)}\cdot$Ag(I) were replaced with tris(methoxy)benzene groups to simplify the calculations. The twist angle between the two phenyl rings of the biphenylene moiety was set to be –45°.[S3] The U-shaped 2,6-pyridinebis(acylhydrazone) linker unit coordinating with the Ag(I) ion was constructed on the basis of the related crystal structure[S6] and then fully optimized by the DFT calculations using the dispersion corrected B3LYP (B3LYP-D3)[S8] functional with the LANL2DZ (for the Ag(I) ion) and the 6-31G* (for H, C, N, and O atoms) basis sets in *Gaussian 16* software (Gaussian, Inc., Pittsburgh, PA).[S9] Computer resources for the DFT calculations were provided by the Information Technology Center of Nagoya University. The initial model of $\mathbf{3}_{(n=8)}\cdot$Ag(I) was optimized by the MM calculations (Compass II force field) with the geometrical constraints of the Ag(I)-bound linker moieties obtained by the DFT calculations (Fig. S13d, left). In order to estimate the molecular diameter of the self-assembled nanofiber of $\mathbf{3}_{(n=8)}\cdot$Ag(I), helically-stacked tetrameric $\mathbf{3}_{(n=8)}\cdot$Ag(I) ($(\mathbf{3}_{(n=8)}\cdot\mathrm{Ag(I)})_4$) was then constructed according to the following procedures: the energy-minimized $\mathbf{3}_{(n=8)}\cdot$Ag(I) was allowed to manually construct a tetramer $(\mathbf{3}_{(n=8)}\cdot\mathrm{Ag(I)})_4$ with a twisting angle of –30º between the adjacent $\mathbf{3}_{(n=8)}\cdot$Ag(I) foldamers so as to helically stack each other. The initial model of $(\mathbf{3}_{(n=8)}\cdot\mathrm{Ag(I)})_4$ was optimized by the MM calculations (Compass II force field) with the geometrical constraints of the Ag(I)-bound linker moieties (Fig. S13d, right).

Supporting Data

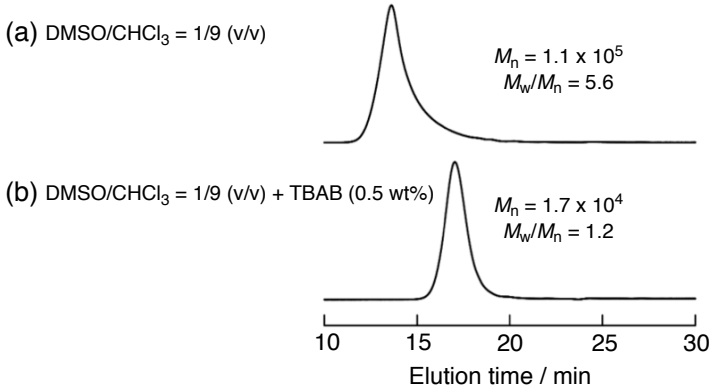

Fig. S1 UV (324 nm) detected SEC chromatograms of **3.** SEC conditions: column, TSKgel G4000H_{HR} (0.78 (i.d.) × 30 cm); eluent, DMSO/$CHCl_3$ (1/9, v/v) (a) and DMSO/$CHCl_3$ (1/9, v/v) containing TBAB (0.5 wt%) (b); flow rate, 0.4 mL/min; column temperature, 50 °C.

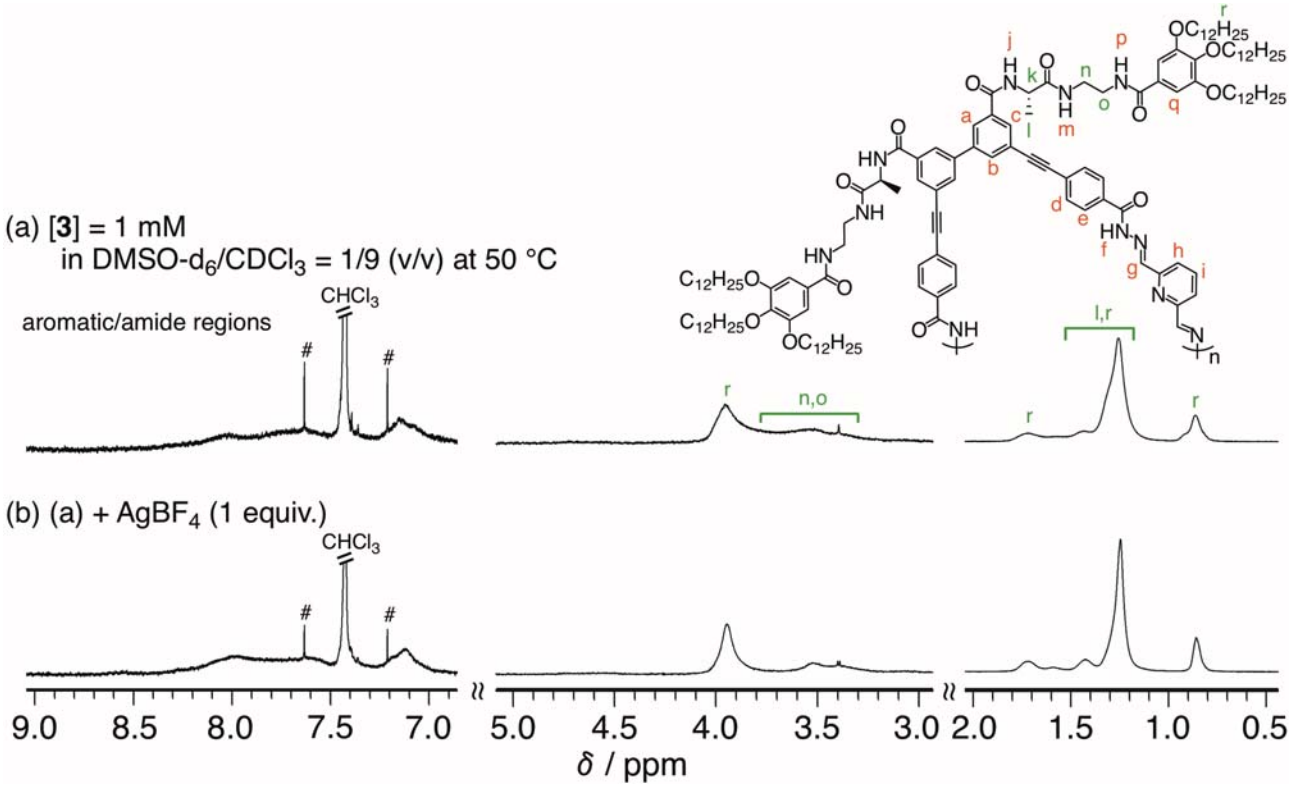

Fig. S2 Partial ^{1}H NMR spectra (500 MHz, DMSO-d_6/$CDCl_3$ (1/9, v/v), 1.0 mM, 50 °C) of **3** (a) and (a) + $AgBF_4$ (1 equiv.) (b). # denotes the ^{13}C satellite peaks of the solvent.

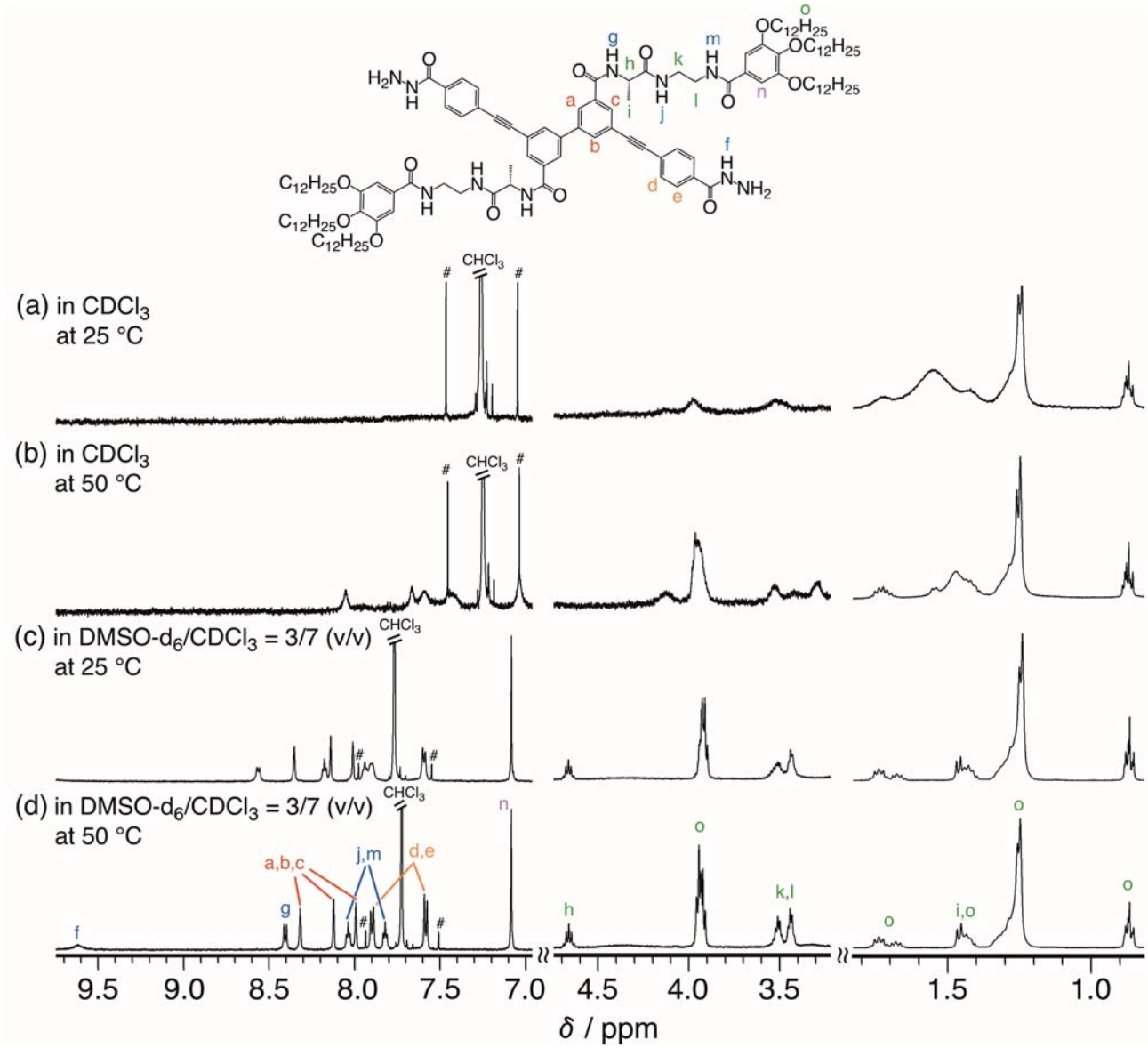

Fig. S3 Partial ^{1}H NMR spectra (500 MHz, 0.4 mM) of **1** in $CDCl_3$ (a,b) at 25 (a) and 50 °C (b) and in DMSO-d_6/$CDCl_3$ (3/7, v/v) (c,d) at 25 (c) and 50 °C (d). # denotes the ^{13}C satellite peaks of the solvent.

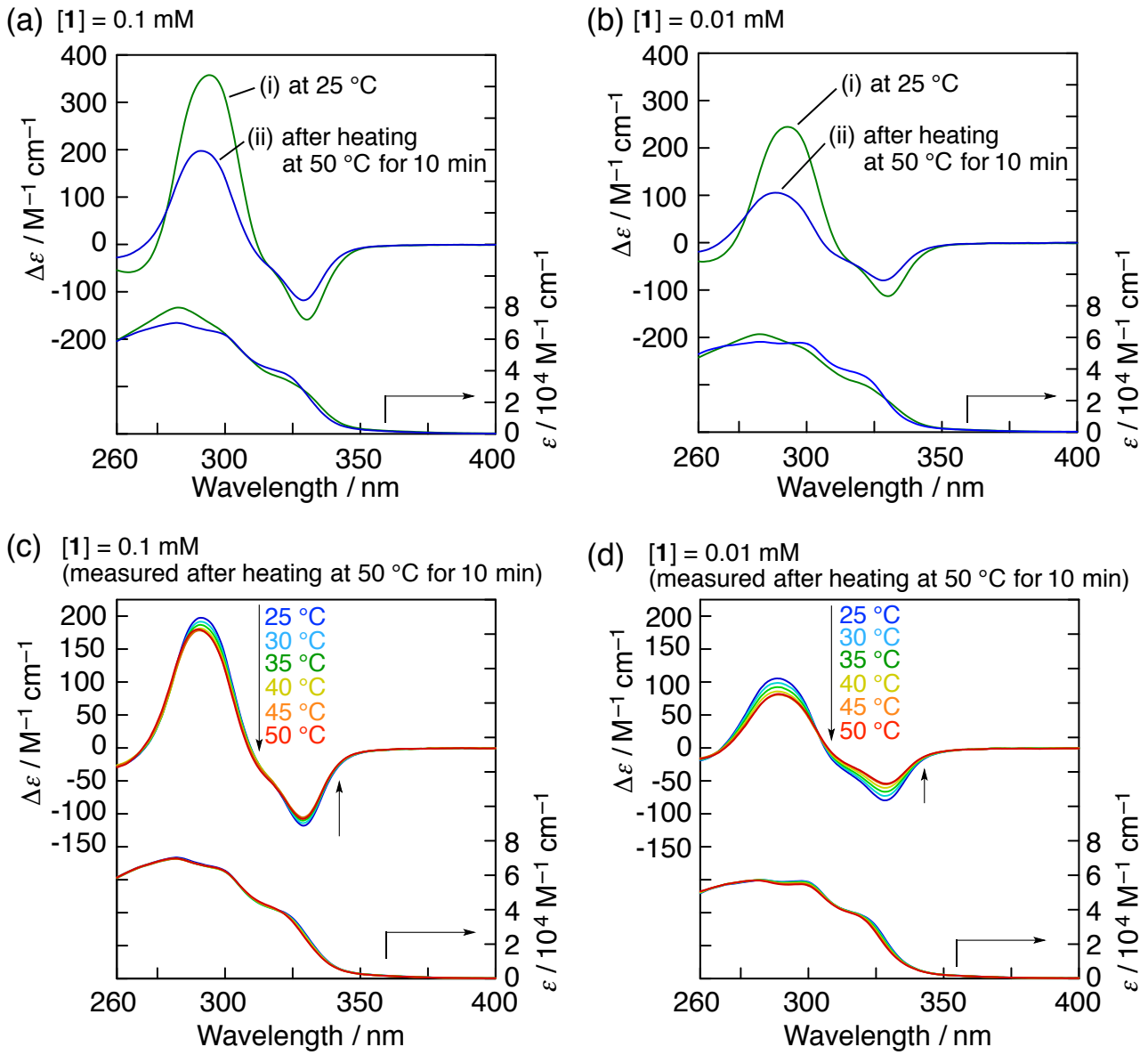

Fig. S4 (a) CD and absorption spectra ($CHCl_3$, 25 °C) of **1** (0.1 mM (a), 0.01 mM (b)) before (i) and after heating at 50 °C for 10 min (ii). These measurements were performed by the following procedures; solutions of **1** (0.1 and 0.01 mM) in $CHCl_3$ were prepared at room temperature and their CD and absorption spectra were measured at 25 °C within 30 min (i). The solutions were then heated at 50 °C for 10 min until reaching an equilibrium state. After cooling to 25 °C, the CD and absorption spectra were measured (ii). Fig. S4a is identical to Fig. 2a. (c,d) Temperature-dependent CD and absorption spectral changes of **1** (0.1 mM (c), 0.01 mM (d)) in $CHCl_3$. These measurements were carried out after heating the $CHCl_3$ solutions of **1** at 50 °C for 10 min.

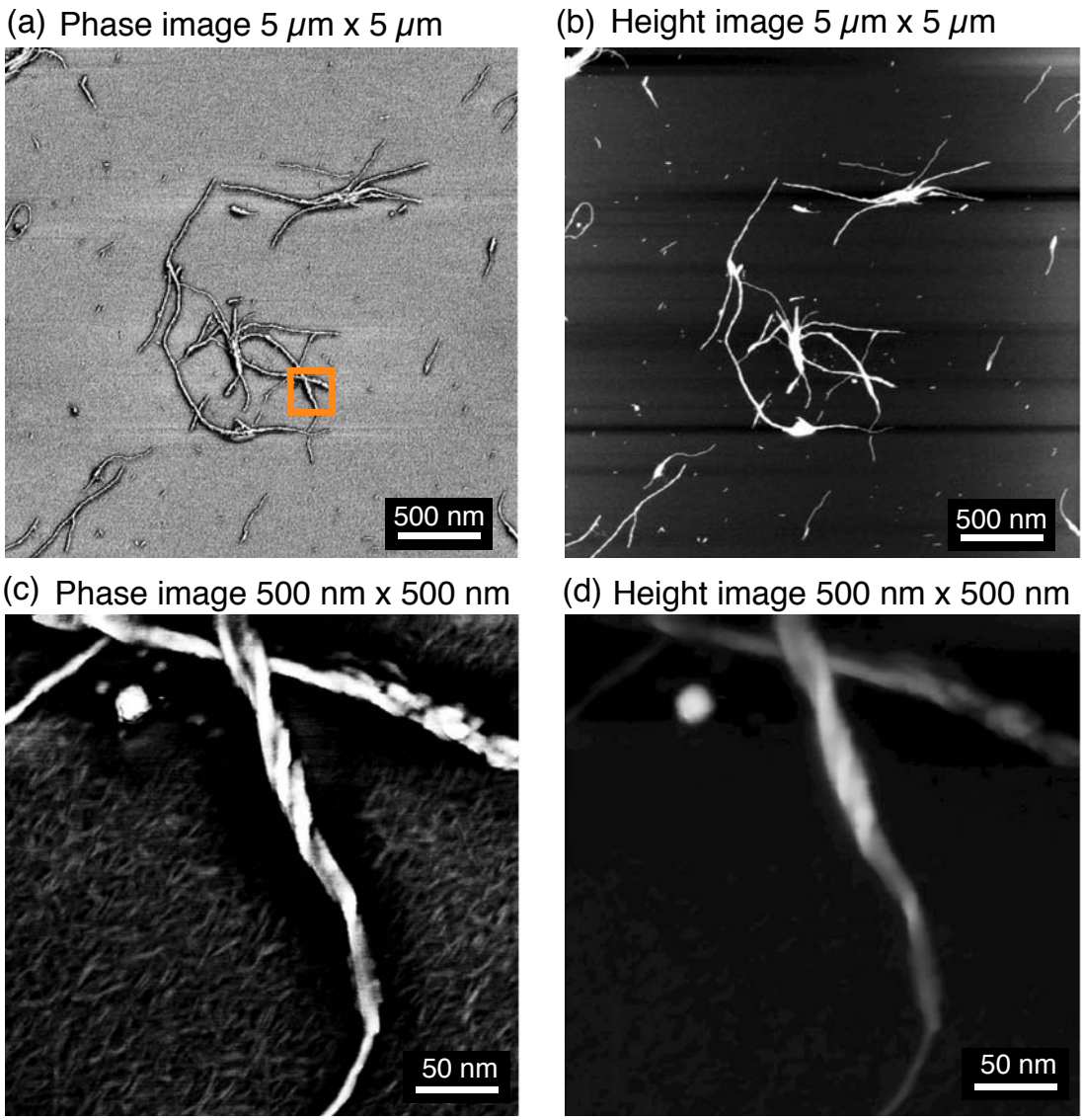

Fig. S5 AFM observation of **1** on mica cast from a dilute $CHCl_3$ solution (0.02 mg mL^{-1}). AFM phase (a and c) and height (b and d) images of **1**. The magnified AFM phase image (c) corresponds to the area indicated by the square in (a).

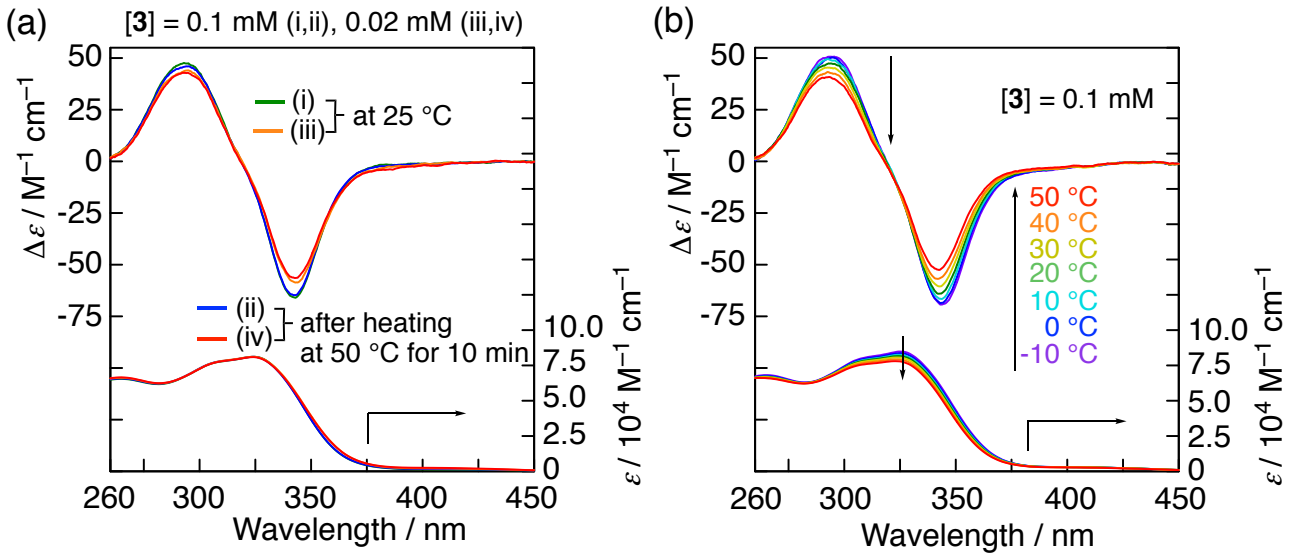

Fig. S6 (a) CD and absorption spectra (DMSO/$CHCl_3$ (1/9, v/v), 0.1 mM per monomer unit (i,ii), 0.02 mM per monomer unit (iii,iv), 25 °C) of **3** before (i,iii) and after heating at 50 °C for 10 min (ii,iv). Solutions of **3** (0.1 and 0.02 mM) were prepared in a DMSO/$CHCl_3$ mixture (1/9, v/v) at room temperature and their CD and absorption spectra were measured at 25 °C within 30 min (i,iii), which were then heated at 50 °C for 10 min. After cooling to 25 °C, the CD and absorption spectra were measured (ii,iv). (b) Temperature-dependent CD and absorption spectral changes (DMSO/$CHCl_3$ (1/9, v/v), 0.1 mM per monomer unit) of **3**.

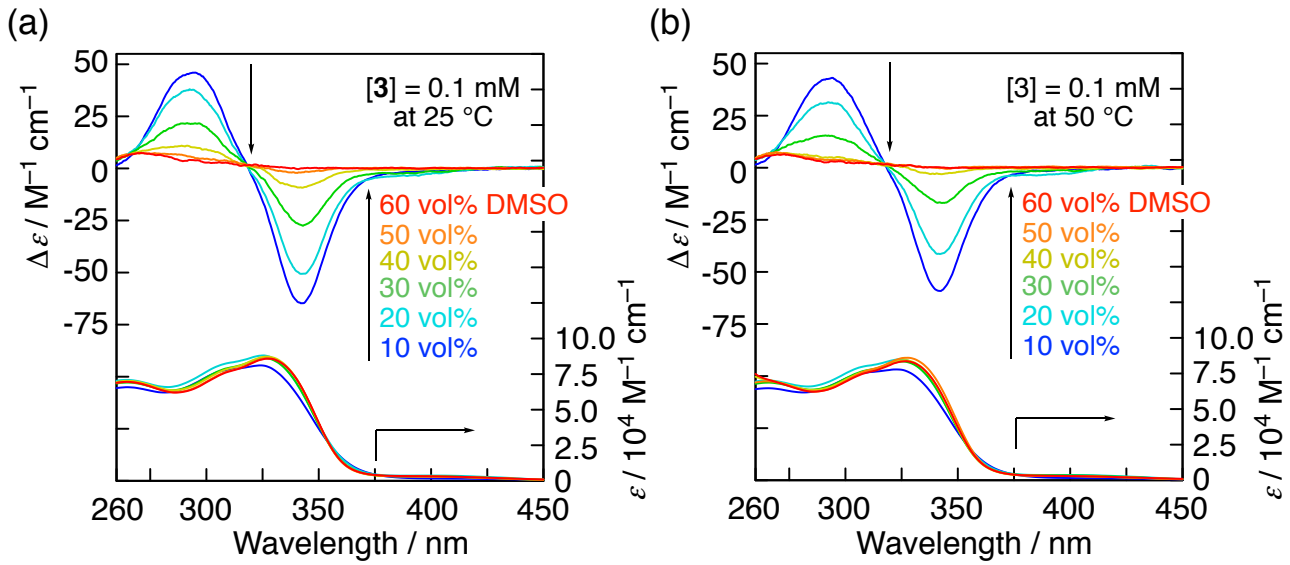

Fig. S7 CD and absorption spectra of **3** (0.1 mM) in various DMSO/$CHCl_3$ mixtures (v/v) at 25 (a) and 50 °C (b).

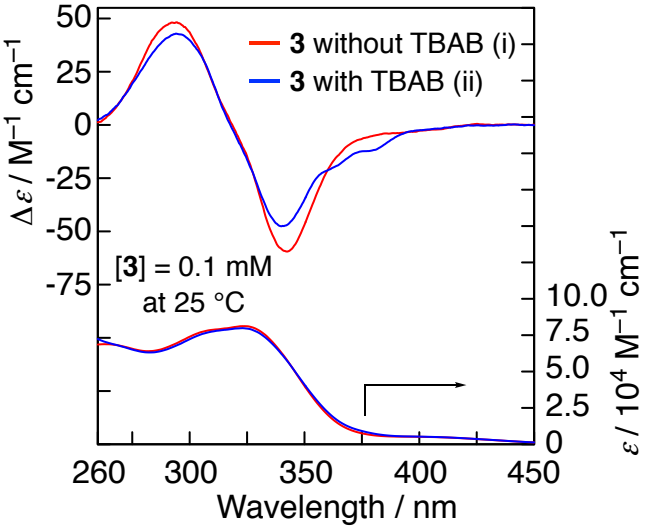

Fig. S8 CD and absorption spectra (0.1 mM per monomer unit, 25 °C) of **3** in DMSO/$CHCl_3$ (1/9, v/v) (i) and DMSO/$CHCl_3$ (1/9, v/v) containing TBAB (0.5 wt% (22 mM)) (ii). The CD and absorption spectra of **3** were measured at 25 °C after heating the solutions at 50 °C for 10 min.

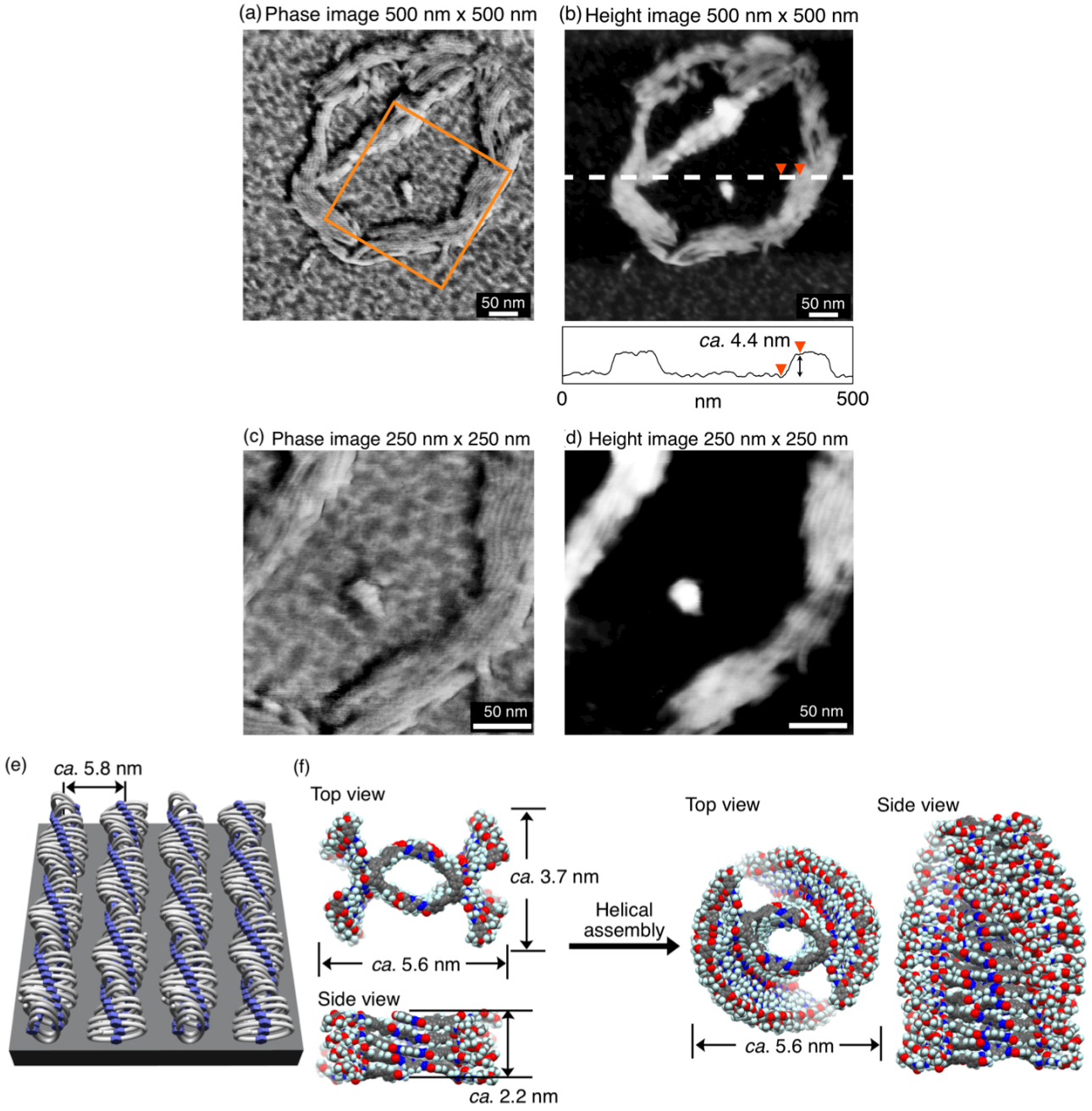

Fig. S9 (a-d) AFM observation of **3** on mica cast from a dilute DMSO/$CHCl_3$ (*ca.* 2/98, v/v) solution (0.04 mg mL^{-1}). AFM phase (a and c) and height (b and d) images of **3**. The cross-sectional profile denoted by the white dashed line is also shown in (b). The magnified AFM phase (c) and height (d) images correspond to the area indicated by the square in (a). (e) Schematic representation of a possible bundle structure of supramolecular helical assemblies of **3** on mica. The blue color represents the W-shaped linker units. (f) Top and side views of the molecular models of foldamer $\mathbf{3}_{(n=8)}$ (octamer of **3**) (left) and its tetrameric helical assembly ($(\mathbf{3}_{(n=8)})_4$) (right). For simplicity, the dodecyloxy chains were replaced with methoxy groups.

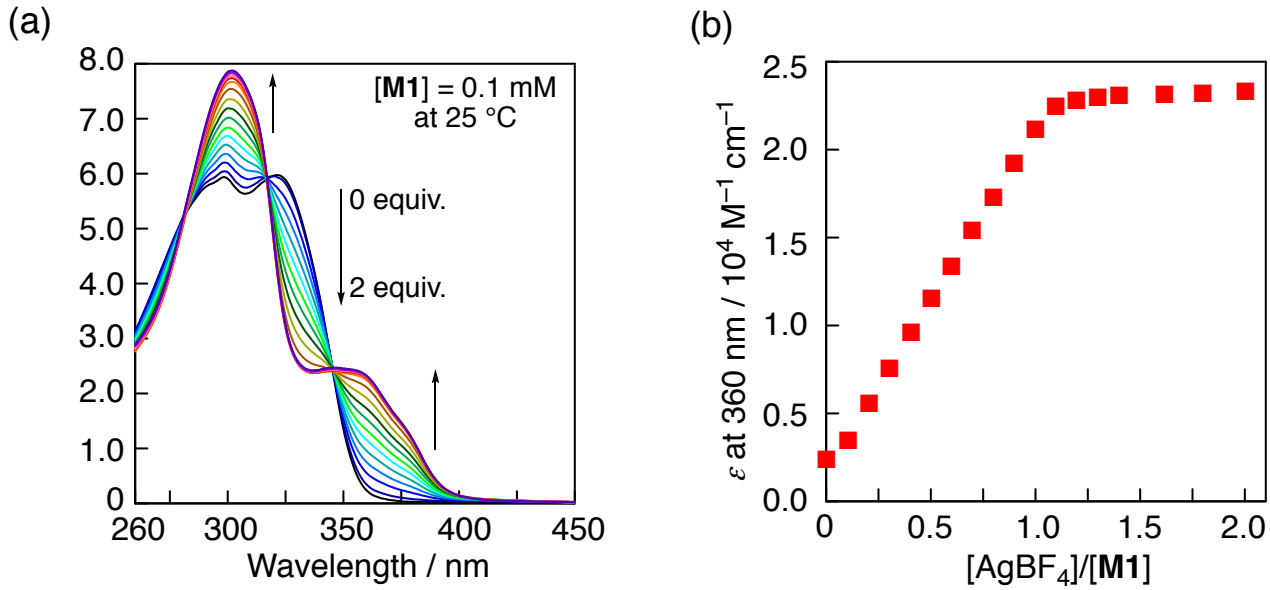

Fig. S10 (a) UV–vis titrations of **M1** (DMSO/$CHCl_3$ (1/9, v/v), 0.1 mM, 25 °C) with $AgBF_4$. (b) Plots of ε at 360 nm for **M1** as a function of [$AgBF_4$]/[**M1**] at 25 °C.

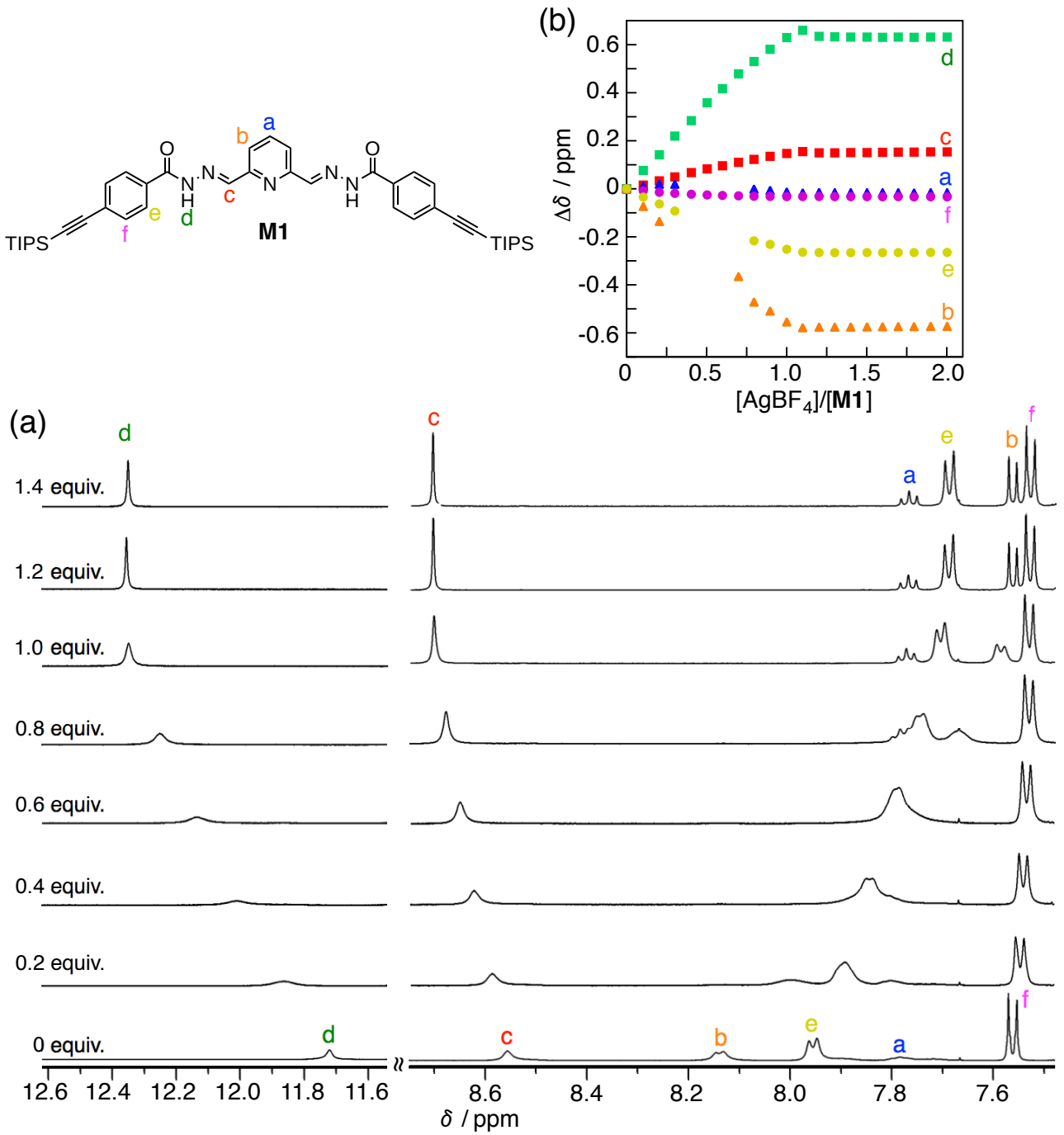

Fig. S11 (a) ^{1}H NMR (500 MHz, DMSO-d_6/$CDCl_3$ (1/9, v/v), 25 °C) spectral changes of **M1** (3.0 mM) in the presence of $AgBF_4$ (0–1.4 equiv.). (b) Plots of chemical shift changes ($\Delta\delta$) for **M1** as a function of [$AgBF_4$]/[**M1**].

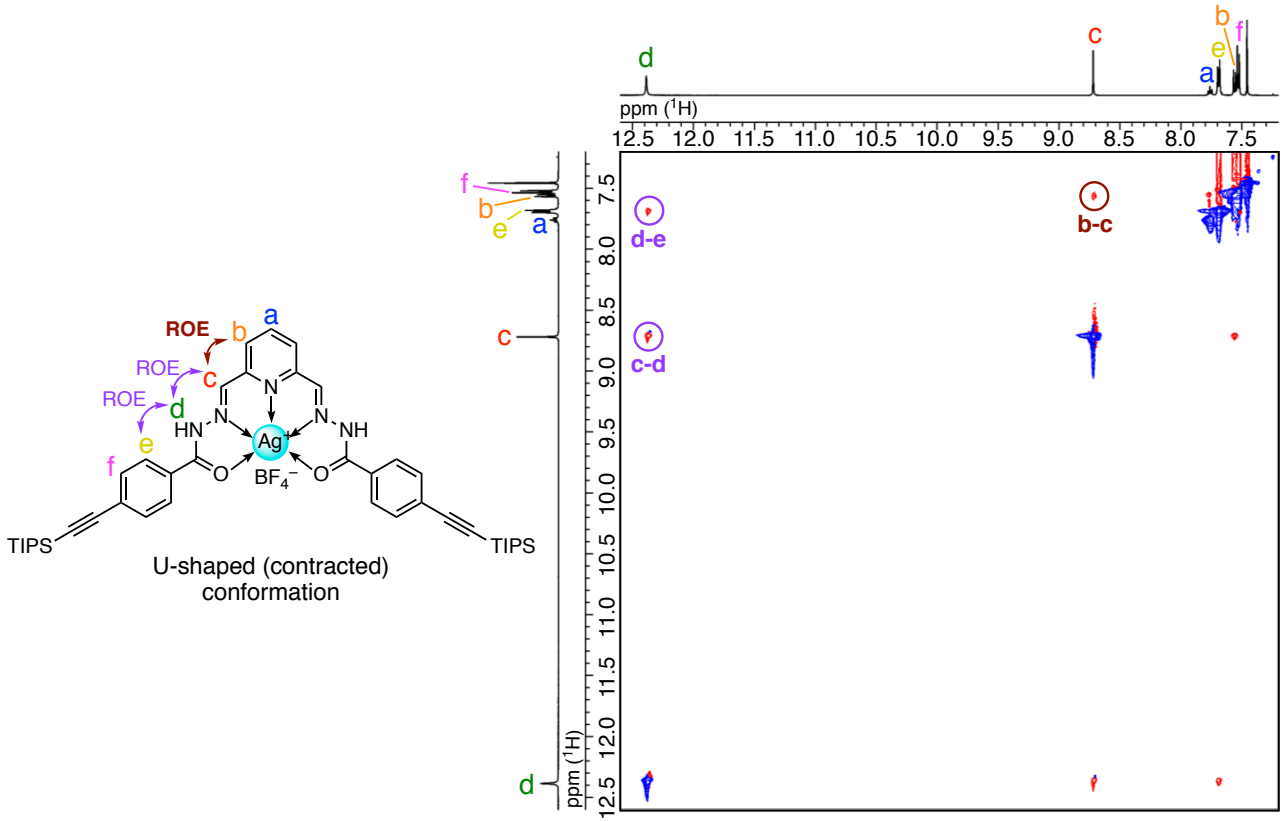

Fig. S12 Partial ROESY (500 MHz, 3.0 mM, DMSO-d_6/$CDCl_3$ (1/9, v/v), 25 °C, mixing time = 0.2 sec) spectrum of **M1** in the presence of 1.4 equiv. of $AgBF_4$.

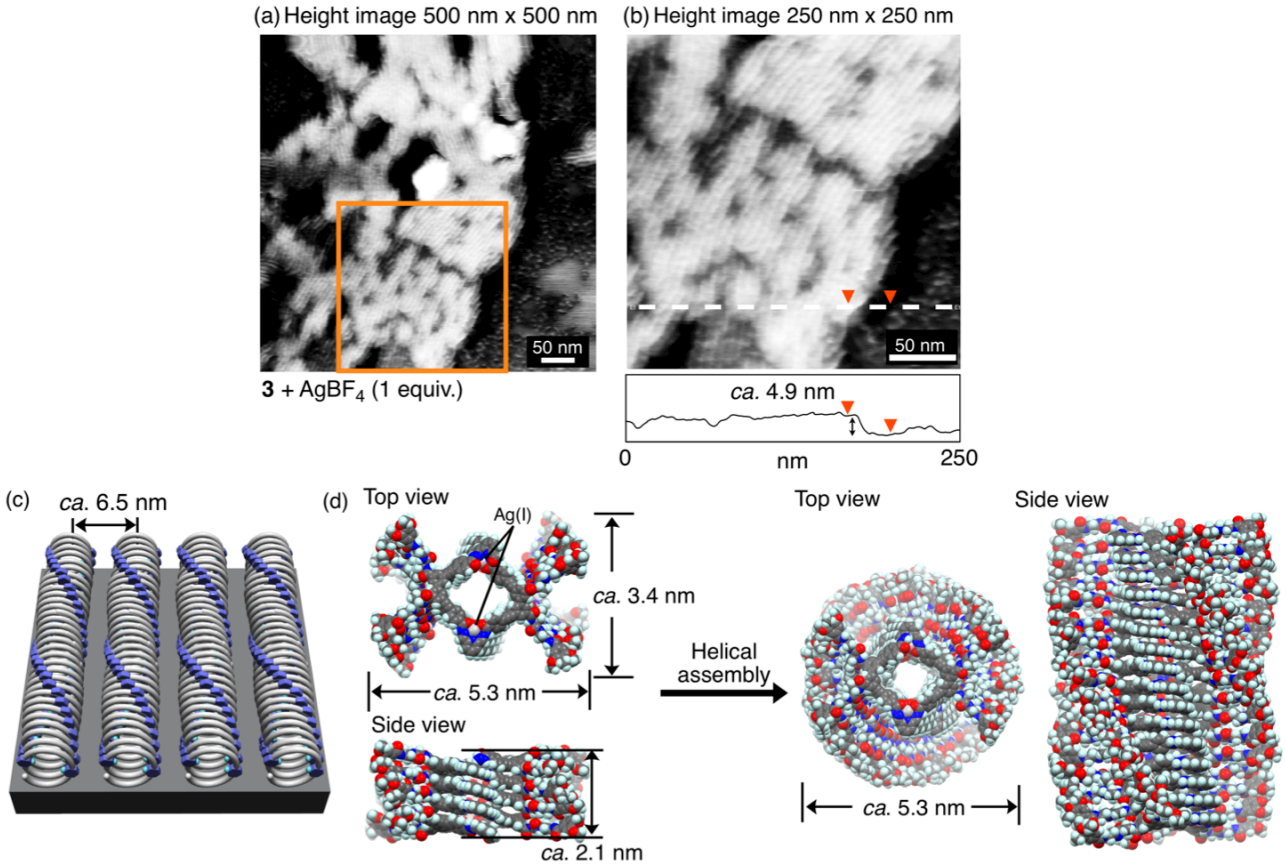

Fig. S13 (a,b) AFM observation of **3** in the presence of $AgBF_4$ (1 equiv.) on mica cast from a dilute DMSO/$CHCl_3$ (*ca.* 1/99, v/v) solution (0.02 mg mL^{-1}). AFM height (a and b) images of **3** in the presence of $AgBF_4$ (1 equiv.). The cross-sectional profile denoted by the white dashed line is also shown in (b). The magnified AFM height image (b) correspond to the area indicated by the square in (a). (c) Schematic representation of a possible bundle structure of supramolecular helical assemblies of **3** in the presence of $AgBF_4$ (1 equiv.) on mica. The blue color represents the U-shaped linker units. (d) Top and side views of the molecular models of foldamer Ag(I)-bound $\mathbf{3}_{(n=8)}$ ($\mathbf{3}_{(n=8)}$·Ag(I)) (left) and its tetrameric helical assembly ($\mathbf{3}_{(n=8)}$·Ag(I))$_4$ (right). For simplicity, the dodecyloxy chains were replaced with methoxy groups.

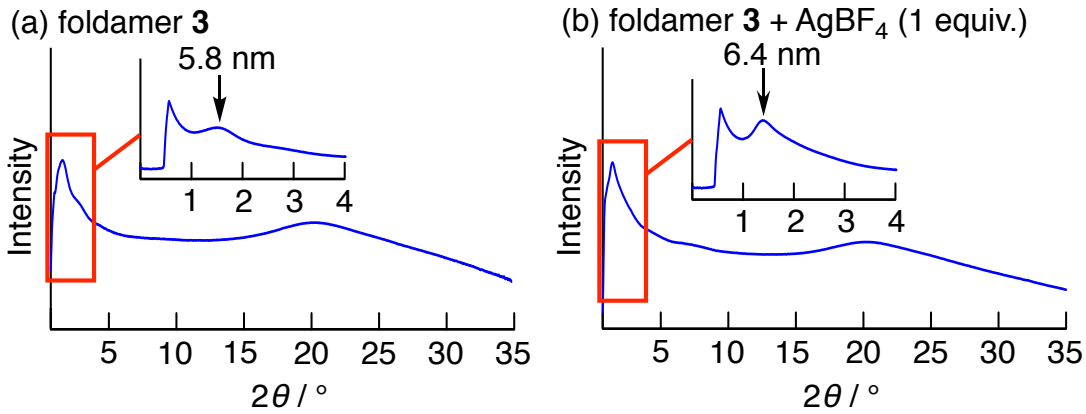

Fig. S14 WAXD and SAXD (inset) profiles of powder samples of **3** (a) and its complex with Ag(I) ions (b). The samples were prepared from each solution (0.1 mM per monomer unit) in DMSO/$CHCl_3$ (1/9, v/v) after evaporation of the solvents.

As anticipated, the WAXD profiles of powder samples of **3**-based supramolecular polymer and its complex with Ag(I) ions exhibited a diffuse halo in the wide-angle region (15~20°, 4–6 Å) probably due to reflections arising from the disordered side-chains and/or hydrogen-bonded stacked repeating units. On the other hand, the **3**-based supramolecular polymer and its complex with Ag(I) ions showed characteristic reflections at 5.8 and 6.4 nm, respectively, in their SAXD profiles, which are in good agreement with the fiber-fiber spacing values observed in the AFM images (5.8 and 6.5 nm, respectively; see Figs. 3b,c, S9 and S13). Although these XRD profiles did not provide exact packing arrangements and helical structural information of **3**-based supramolecular polymer and its complex with Ag(I) ions, the observed XRD measurement results also support tubular-like assembled helical structures of **3**-based supramolecular polymer and its complex with Ag(I) ions as shown in Fig. 1c.

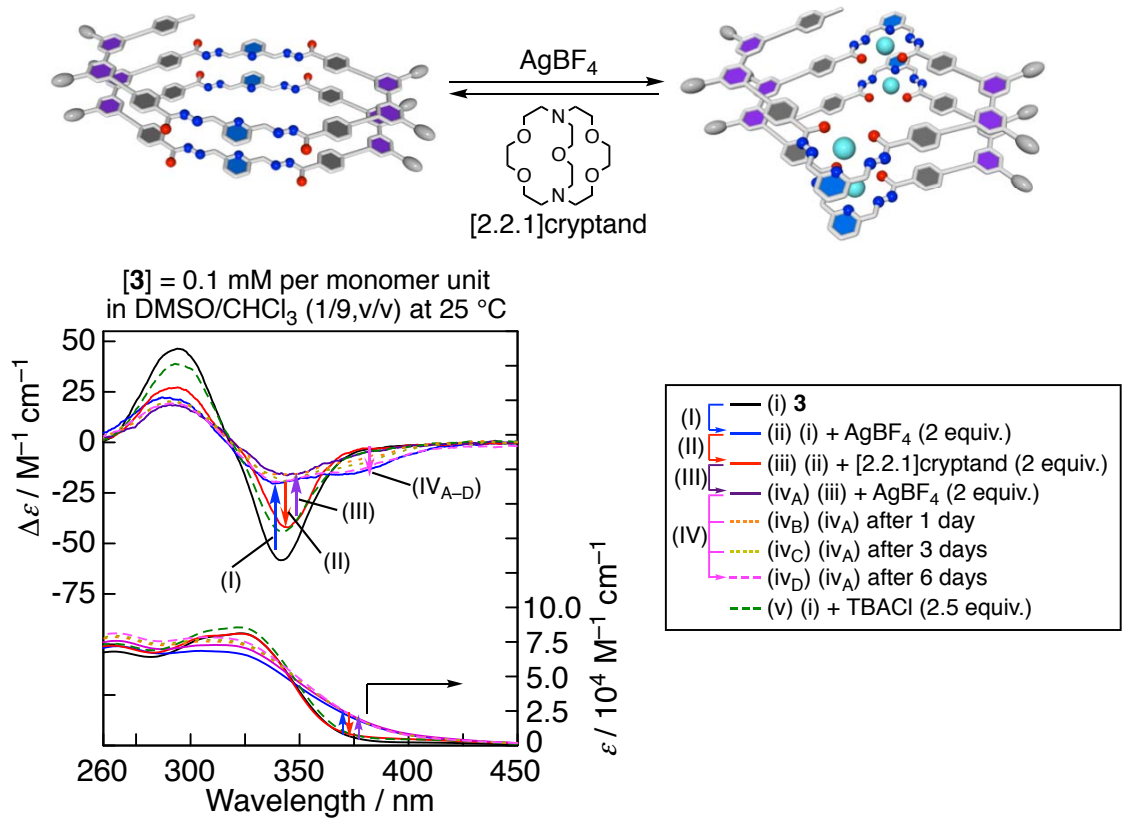

Fig. S15 CD and absorption spectra of **3** ($DMSO/CHCl_3$ (1/9, v/v), 0.1 mM per monomer unit, 25 °C) after heating the solutions at 50 °C for 10 min (i), (i) + $AgBF_4$ (2 equiv.) (ii), (ii) + [2.2.1]cryptand (2 equiv.) (iii), and those just after the further addition of $AgBF_4$ (2 equiv.) (iv_A) followed by standing at 25 °C for 1 (iv_B), 3 (iv_C), and 6 days (iv_D). The CD and absorption spectra of **3** in the presence of TBA chloride (TBACl, 2.5 equiv.) in $DMSO/CHCl_3$ (1/9, v/v) are also shown (v).

In order to demonstrate a reversible helix-to-helix transition of **3** upon the binding and release of Ag(I) ions to the metal-binding linker units of **3**, the CD and absorption spectral changes of **3** were followed by the sequential addition of $AgBF_4$ (2 equiv.) and [2.2.1]cryptand, a strong receptor for Ag(I) ions, in $DMSO/CHCl_3$ (1/9, v/v) at 25 °C. As shown in Fig. S15, the absorption spectrum of **3** complexed with $AgBF_4$ (2 equiv.) (ii) was almost restored to that of **3** after the addition of [2.2.1]cryptand (2.0 equiv.), which trapped the Ag(I) ions from **3**, although the CD intensity of **3** did not recover completely ((i)-(iii)). This is due to a large excess amount of BF_4^- anions that most likely bind to the acylhydrazone NH groups of the linker moieties and/or the oligoamide NH groups of **3** (for an example, see ref S10). In fact, the CD spectrum of **3** complexed with $AgBF_4$ (2 equiv.) after the addition of [2.2.1]cryptand (2.0 equiv.) was similar to that of **3** in the presence of TBACl (2.5 equiv.) ((iii) and (v)). Upon the further addition of $AgBF_4$ (2 equiv.), the CD and absorption

spectra gradually changed with time (iv_A–iv_D) and were almost switched back to the original ones (ii) after six days (iv_D). The observed time-dependent CD intensity changes can be ascribed to an excess amount of BF_4^- anions binding to the pendant NH groups of **3** as mentioned above, resulting in dissociation of the self-assembled polymeric **3** into a monomeric or an oligomeric **3** as supported by the SEC experiments of **3** in the presence and absence of TBAB (Fig. S1). Therefore, the resulting monomeric or oligomeric **3** slowly re-assembled into its tubular **3**-based supramolecular polymer upon complexation with Ag(I) ions. Although the remaining anions slightly affect the CD spectral pattern of **3**, such a unique helix-to-helix transition of **3** was found to be reversibly controlled and switched by the sequential addition of $AgBF_4$ (2 equiv.) and [2.2.1]cryptand in an alternate manner.

Supporting References

(S1) D. A. Stone, A. S. Tayi, J. E. Goldberger, L. C. Palmer and S. I. Stupp, *Chem. Commun.*, 2011, **47**, 5702.

(S2) M. Thompson, ArgusLab, Planaria Software LLC, Seattle, WA (1996).

(S3) F. Grein, *J. Phys. Chem. A*, 2002, **106**, 3823-3827.

(S4) (*a*) J. J. P. Stewart, *J. Mol. Model.*, 2007, **13**, 1173-1213; (*b*) J. J. P. Stewart, *Int. J. Quantum Chem.*, 1996, **58**, 133-146.

(S5) J. J. P. Stewart, MOPAC2012, Stewart Computational Chemistry, Colorado Springs, CO, USA, http://openmopac.net/ 2012.

(S6) (*a*) F. Dumitru, Y. M. Legrand, M. Barboiu, E. Petit and A. van der Lee, *Cryst. Growth Des.*, 2009, **9**, 2917-2921; (*b*) L. Ratjen and J.-M. Lehn, *RSC Adv.*, 2014, **4**, 50554-50557.

(S7) H. Sun, Z. Jin, C. Yang, R. L. C. Akkermans, S. H. Robertson, N. A. Spenley, S. Miller and S. M. Todd, *J. Mol. Model.*, 2016, **22**, 47.

(S8) S. Grimme, J. Antony, S. Ehrlich, H. Krieg, *J. Chem. Phys*. **2010**, *132*, 154104.

(S9) Gaussian 16, Revision A.03, M. J. Frisch, G. W. Trucks, H. B. Schlegel, G. E. Scuseria, M. A. Robb, J. R. Cheeseman, G. Scalmani, V. Barone, G. A. Petersson, H. Nakatsuji, X. Li, M. Caricato, A. V. Marenich, J. Bloino, B. G. Janesko, R. Gomperts, B. Mennucci, H. P. Hratchian, J. V. Ortiz, A. F. Izmaylov, J. L. Sonnenberg, D. Williams-Young, F. Ding, F. Lipparini, F. Egidi, J. Goings, B. Peng, A. Petrone, T. Henderson, D. Ranasinghe, V. G. Zakrzewski, J. Gao, N. Rega, G. Zheng, W. Liang, M. Hada, M. Ehara, K. Toyota, R. Fukuda, J. Hasegawa, M. Ishida, T. Nakajima, Y. Honda, O. Kitao, H. Nakai, T. Vreven, K. Throssell, J. A. Montgomery, Jr., J. E. Peralta, F. Ogliaro, M. J. Bearpark, J. J. Heyd, E. N. Brothers, K. N. Kudin, V. N. Staroverov, T. A. Keith, R. Kobayashi, J. Normand, K. Raghavachari, A. P. Rendell, J. C. Burant, S. S. Iyengar, J. Tomasi, M. Cossi, J. M. Millam, M. Klene, C. Adamo, R. Cammi, J. W. Ochterski, R. L. Martin, K. Morokuma, O. Farkas, J. B. Foresman, and D. J. Fox, Gaussian, Inc., Wallingford CT, 2016.

(S10) Y. Choi and J. Kang, *J. Incl. Phenom. Macrocycl. Chem.*, 2014, **79**, 95.

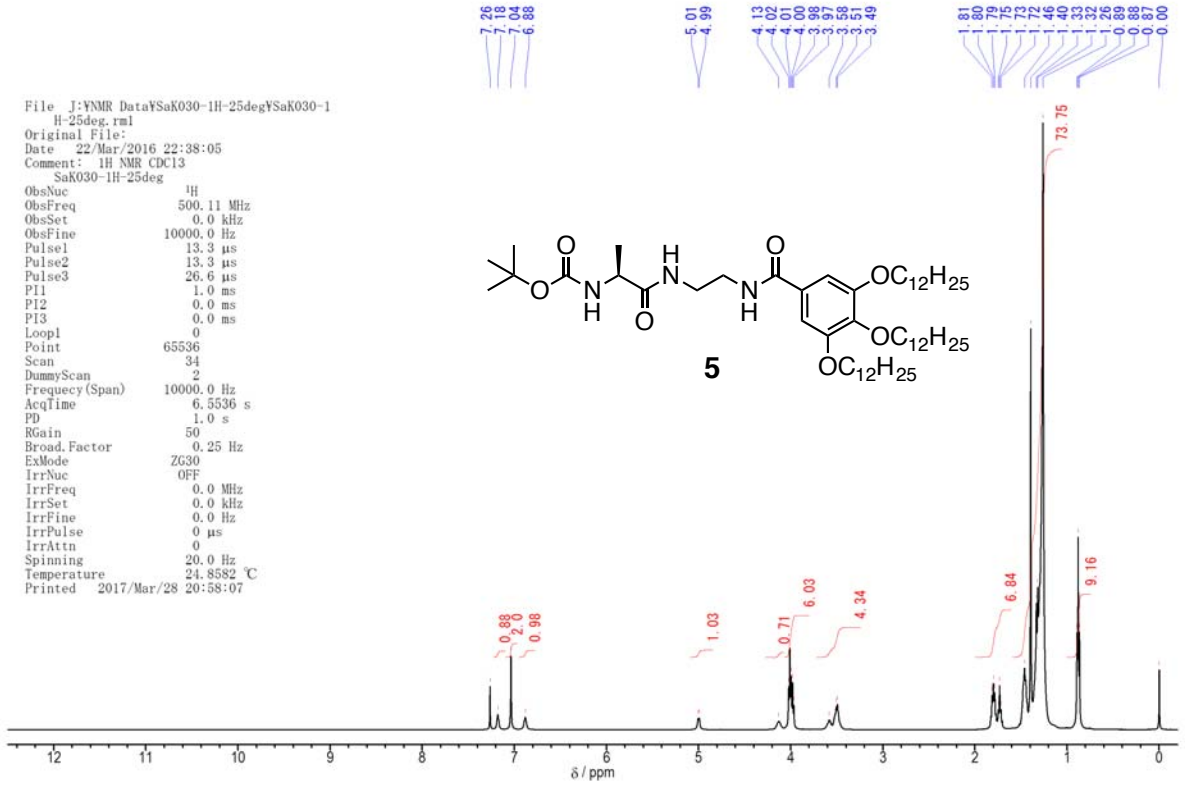

Fig. S16 ^{1}H NMR spectrum of **5** in $CDCl_3$ at 25 ºC.

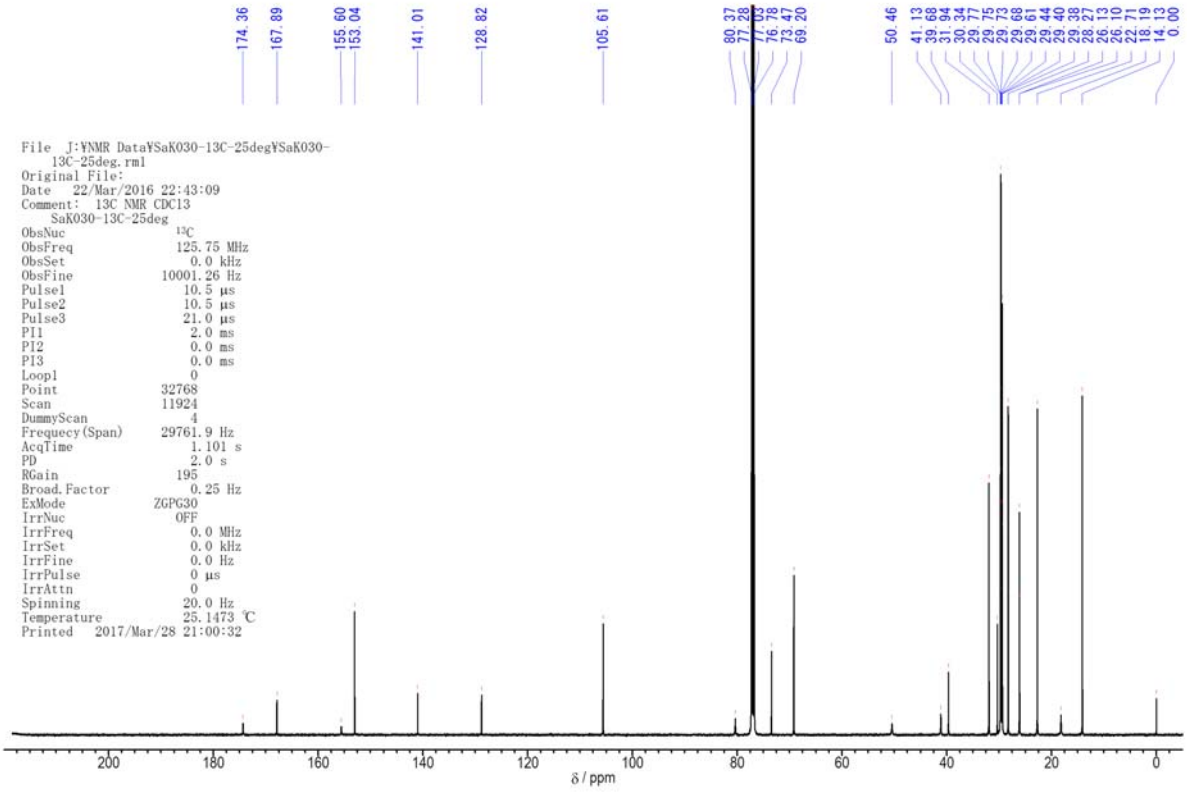

Fig. S17 ^{13}C NMR spectrum of **5** in $CDCl_3$ at 25 ºC.

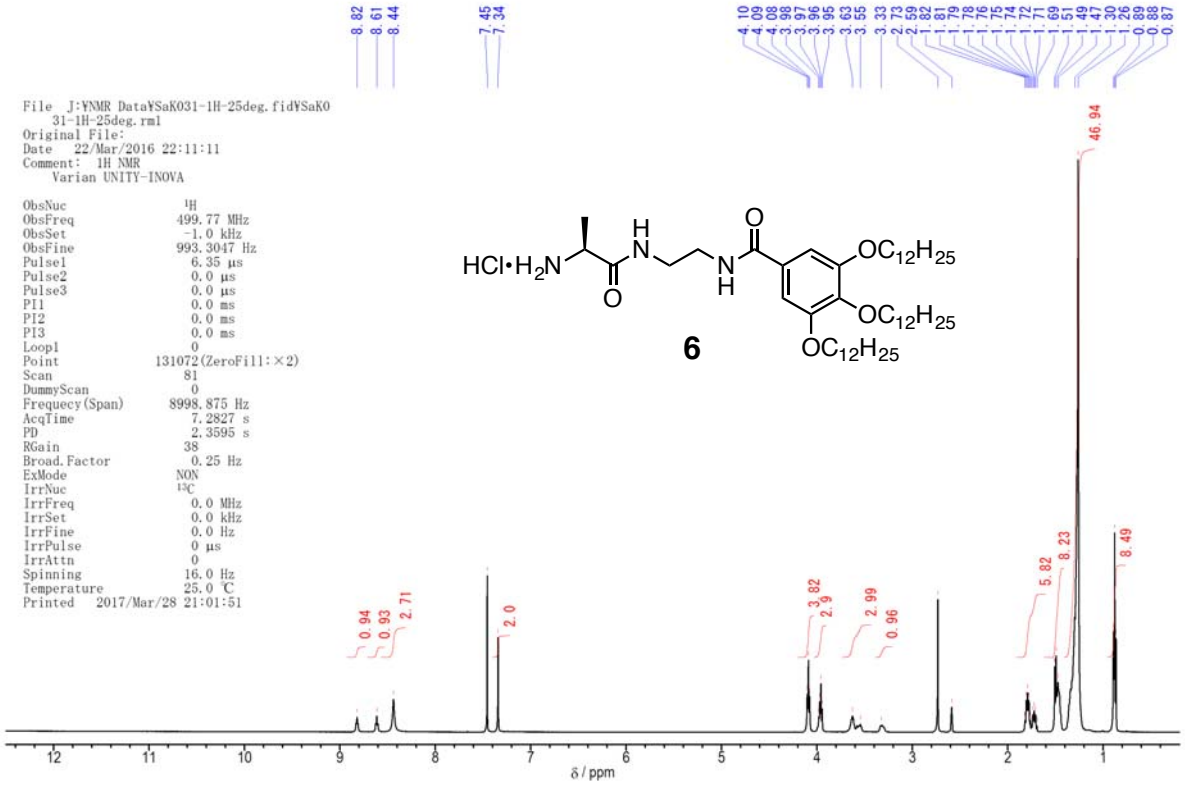

Fig. S18 ^{1}H NMR spectrum of **6** in DMSO-d_6/$CDCl_3$ = 1/9 (v/v) at 25 ºC.

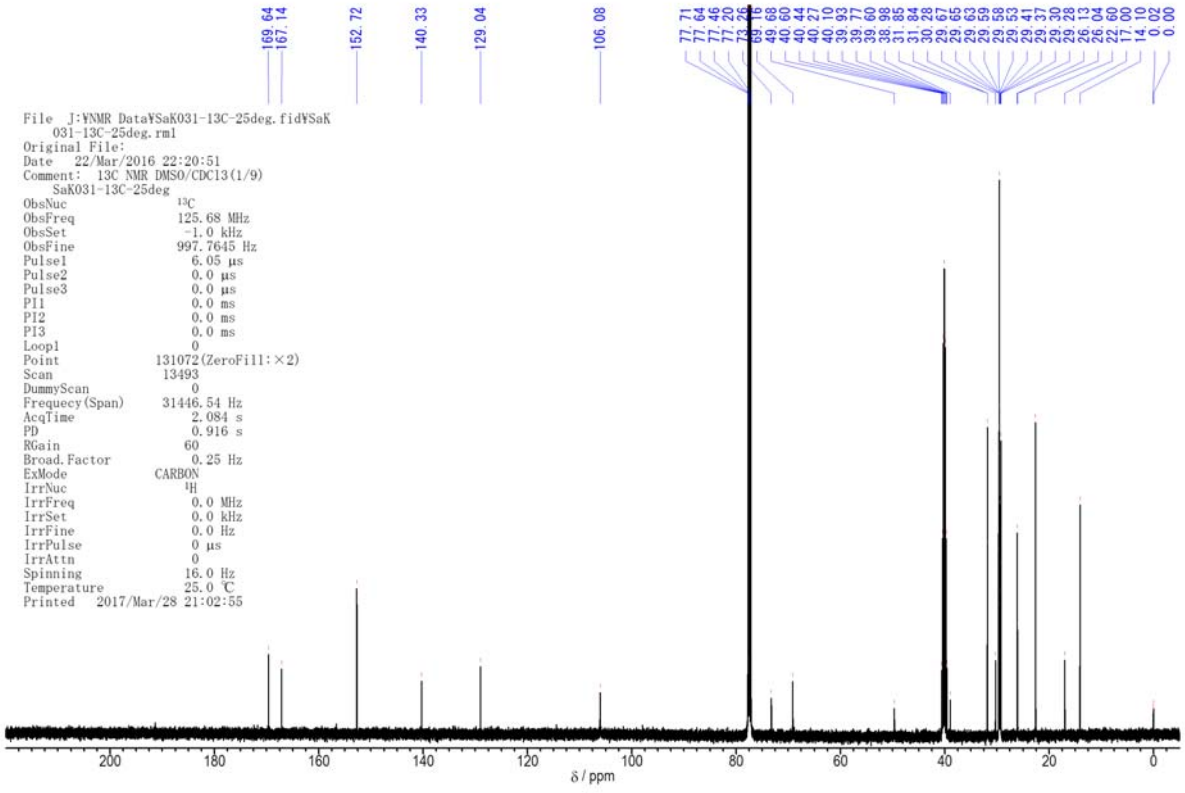

Fig. S19 ^{13}C NMR spectrum of **6** in DMSO-d_6/$CDCl_3$ = 1/9 (v/v) at 25 ºC.

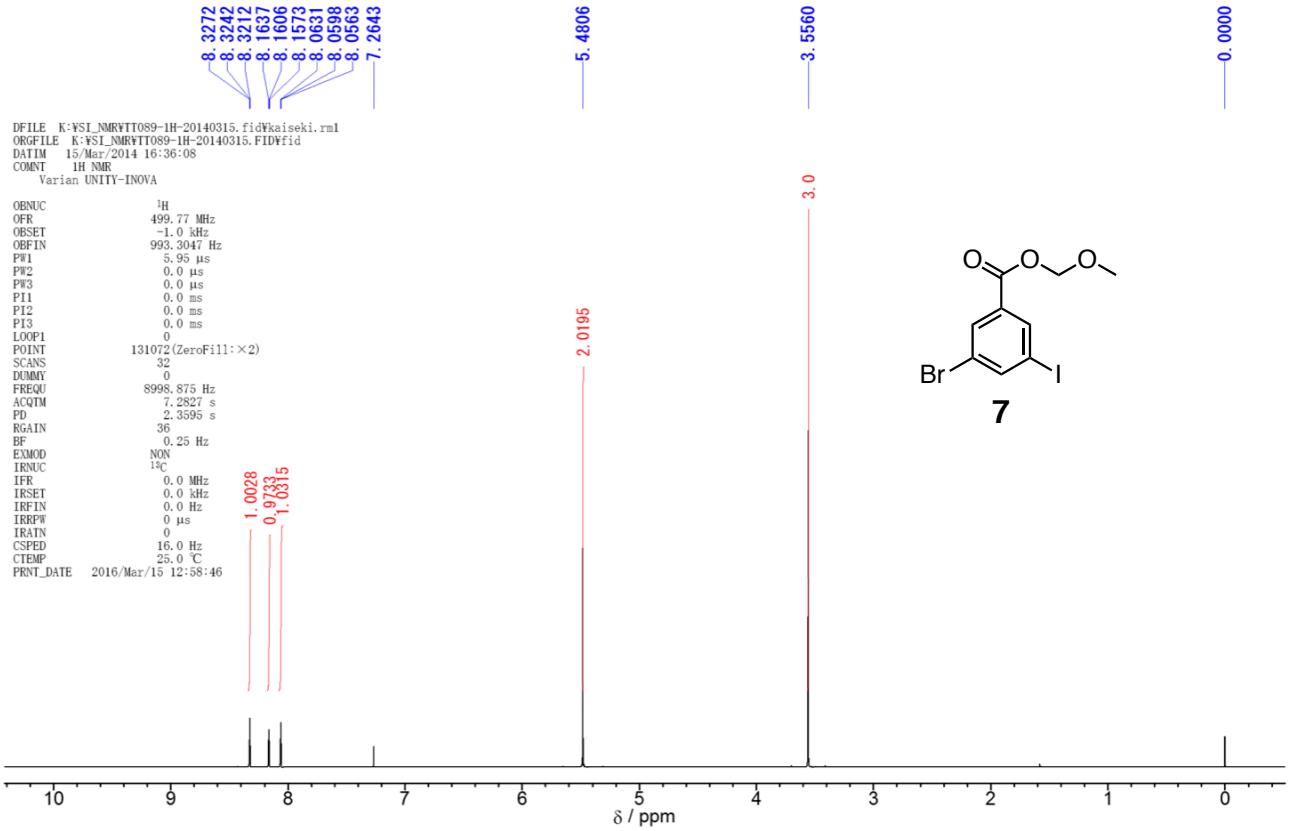

Fig. S20 ^{1}H NMR spectrum of **7** in $CDCl_3$ at 25 ºC.

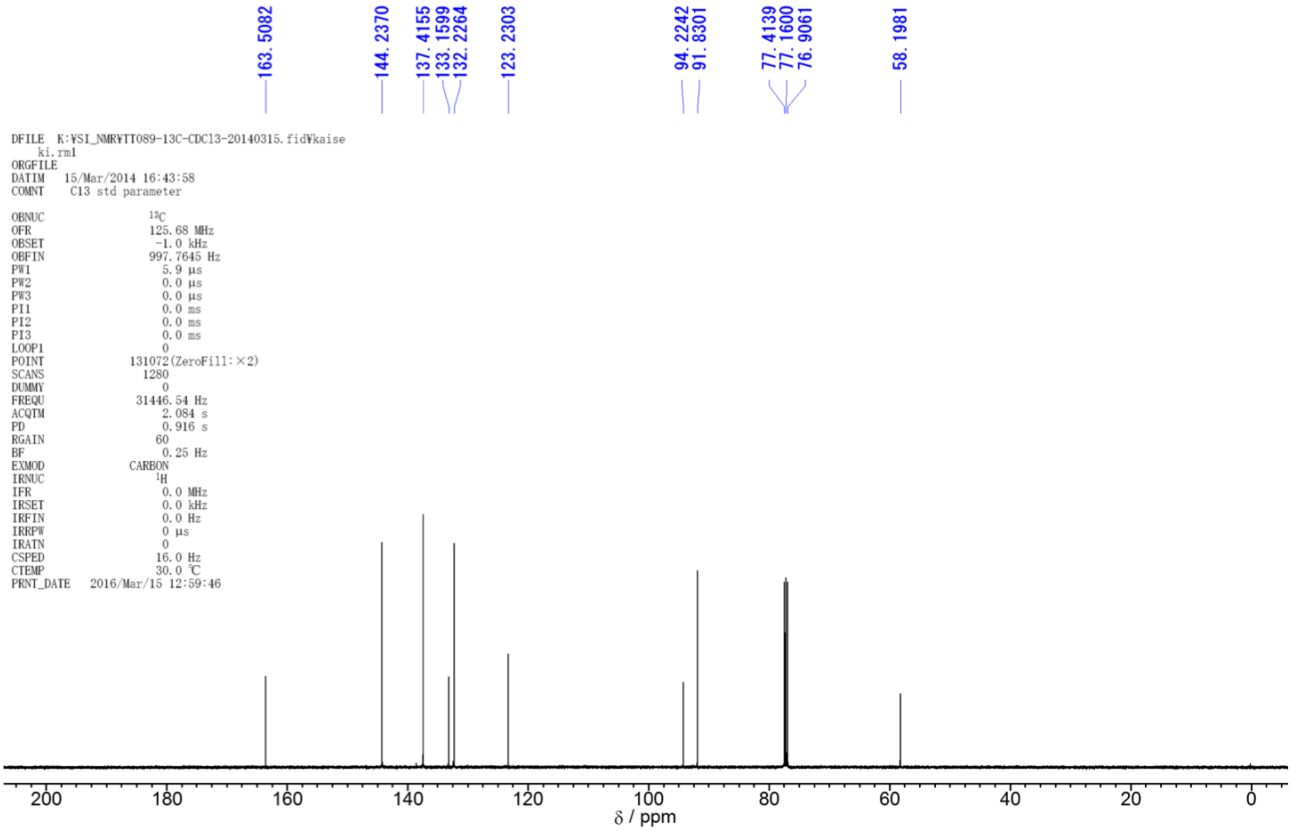

Fig. S21 ^{13}C NMR spectrum of **7** in $CDCl_3$ at 25 ºC.

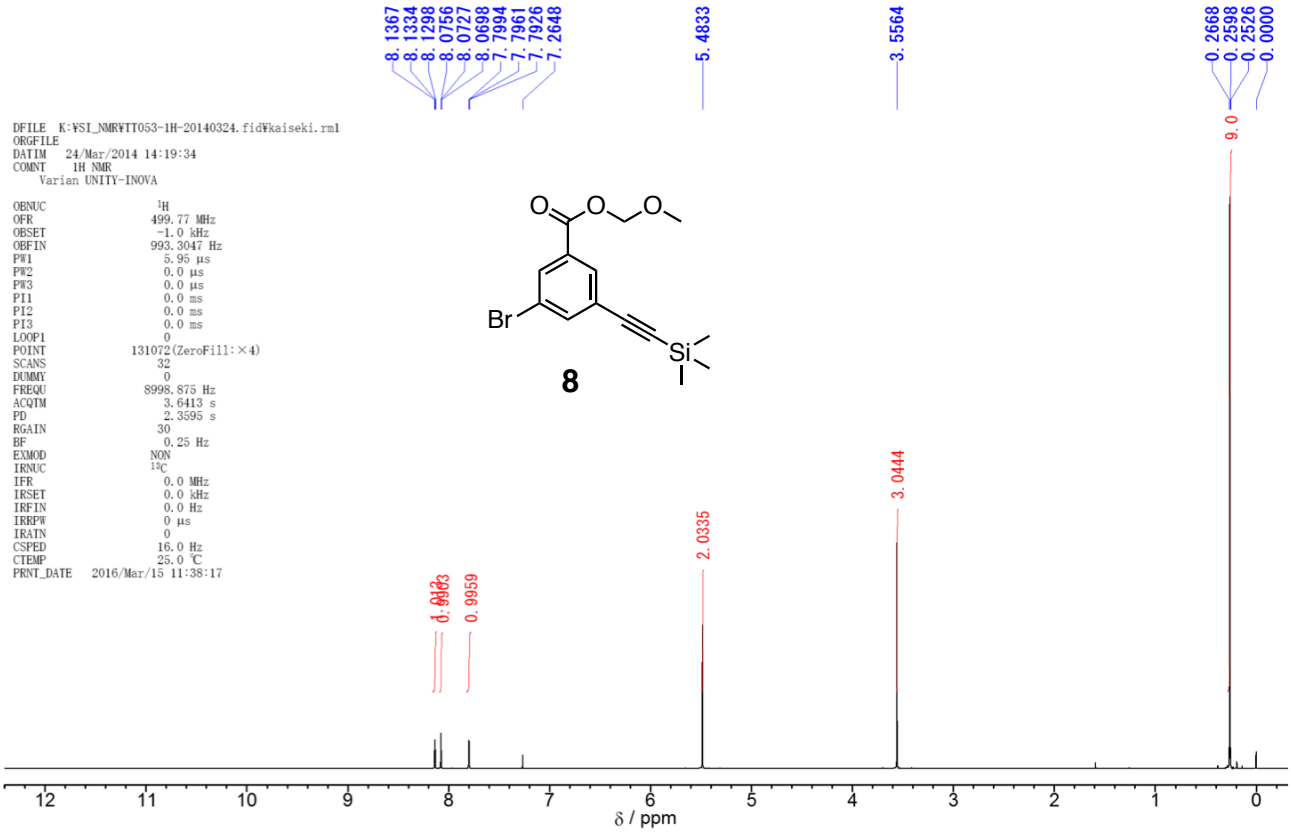

Fig. S22 ^{1}H NMR spectrum of **8** in $CDCl_3$ at 25 ℃.

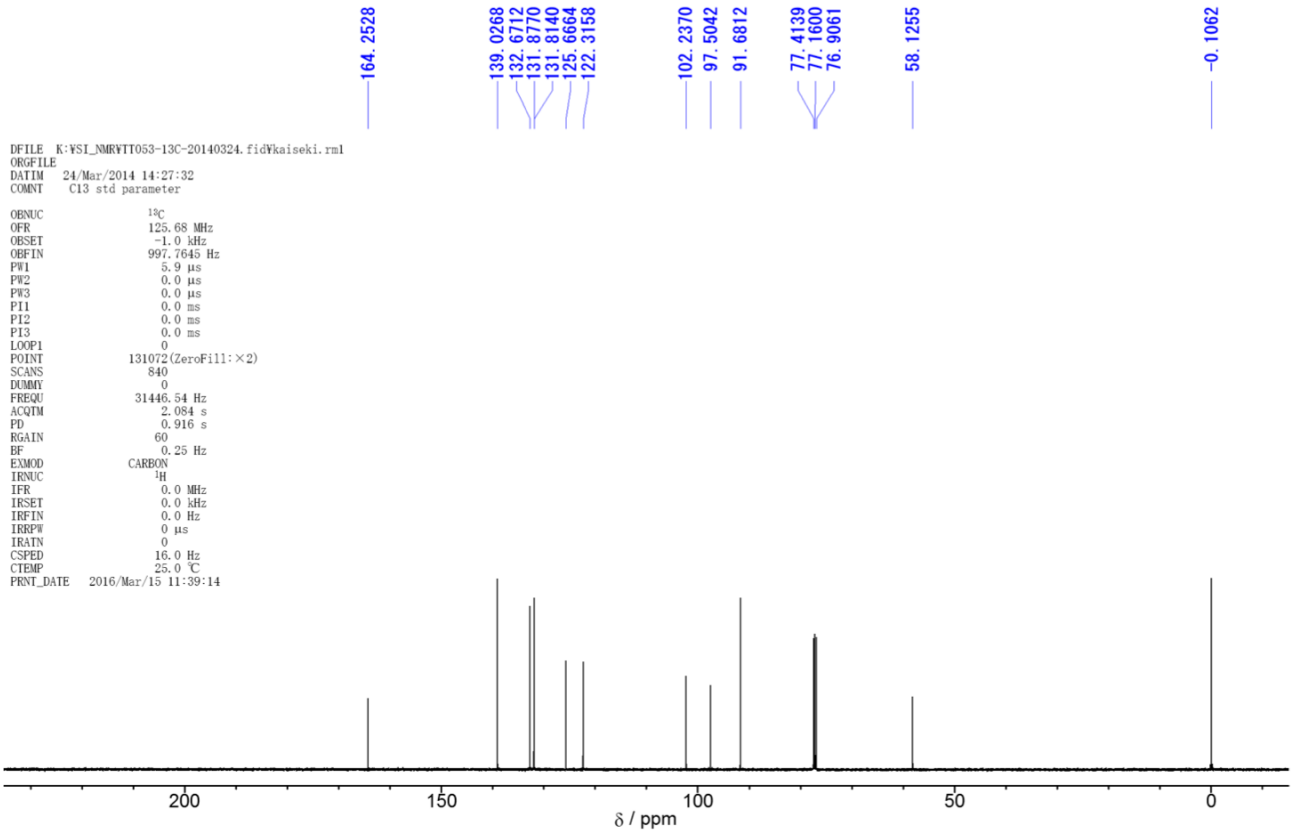

Fig. S23 ^{13}C NMR spectrum of **8** in $CDCl_3$ at 25 ℃.

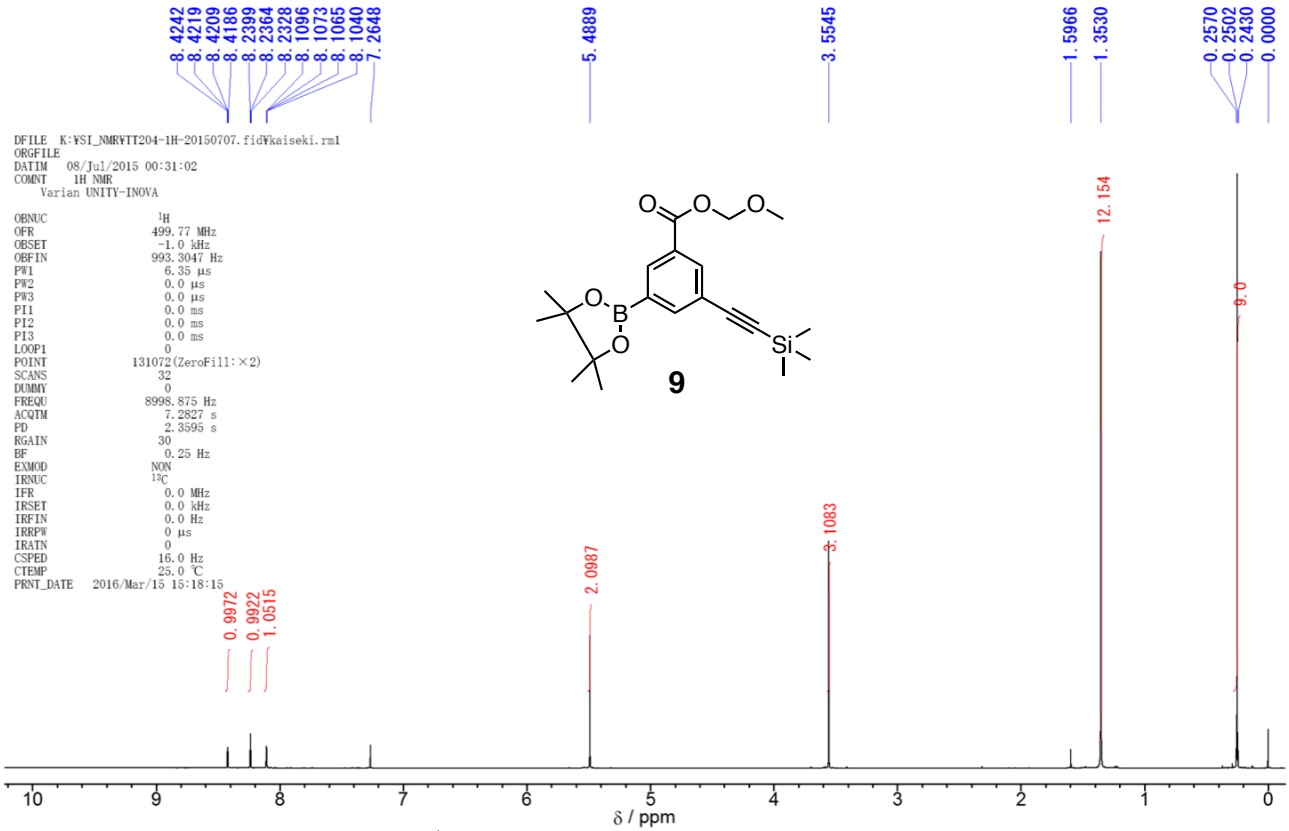

Fig. S24 ^{1}H NMR spectrum of **9** in $CDCl_3$ at 25 ºC.

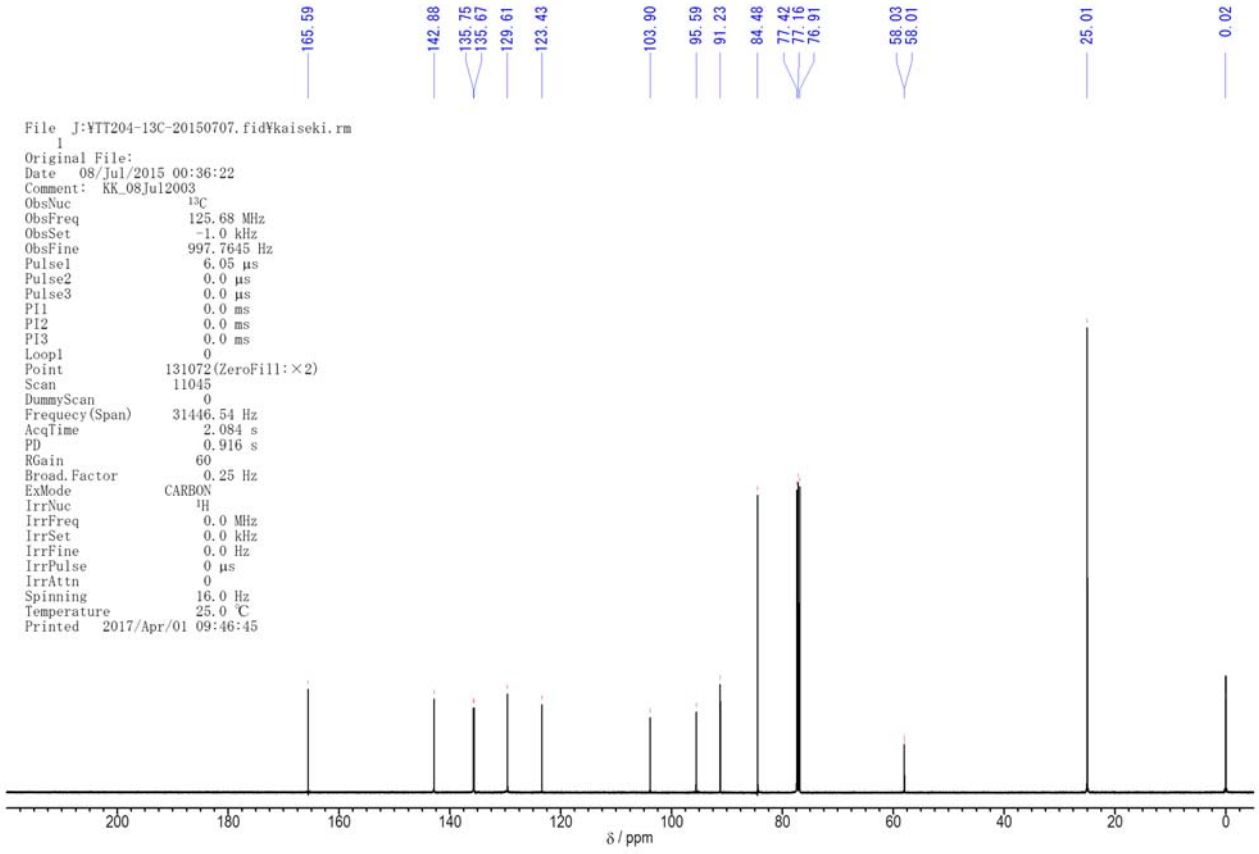

Fig. S25 ^{13}C NMR spectrum of **9** in $CDCl_3$ at 25 ºC.

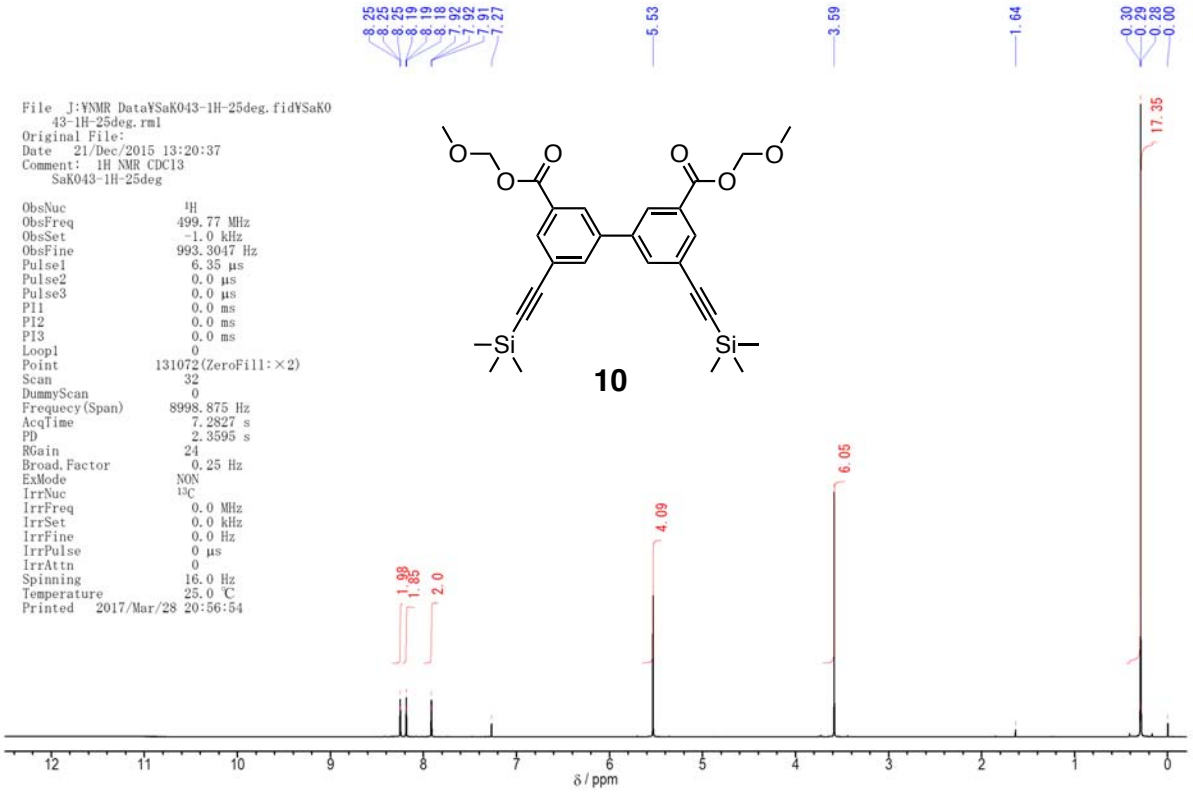

Fig. S26 ^{1}H NMR spectrum of **10** in $CDCl_3$ at 25 ºC.

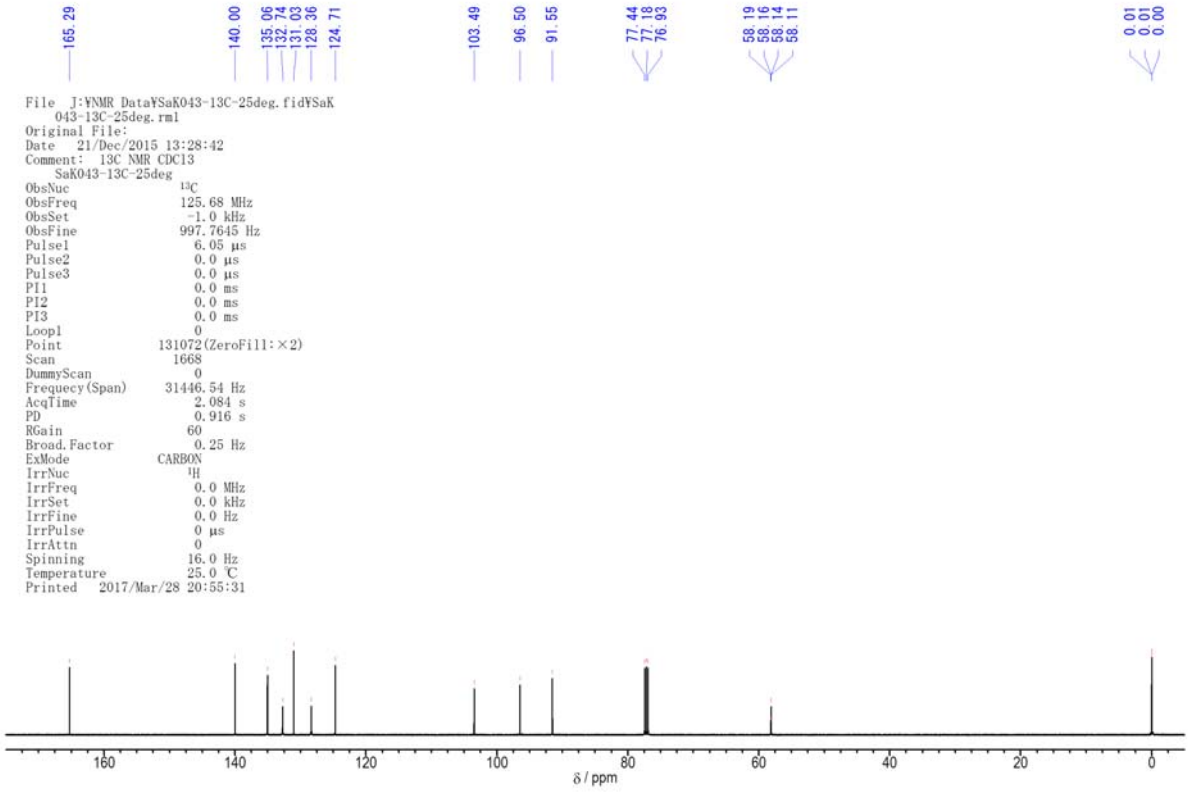

Fig. S27 ^{13}C NMR spectrum of **10** in $CDCl_3$ at 25 ºC.

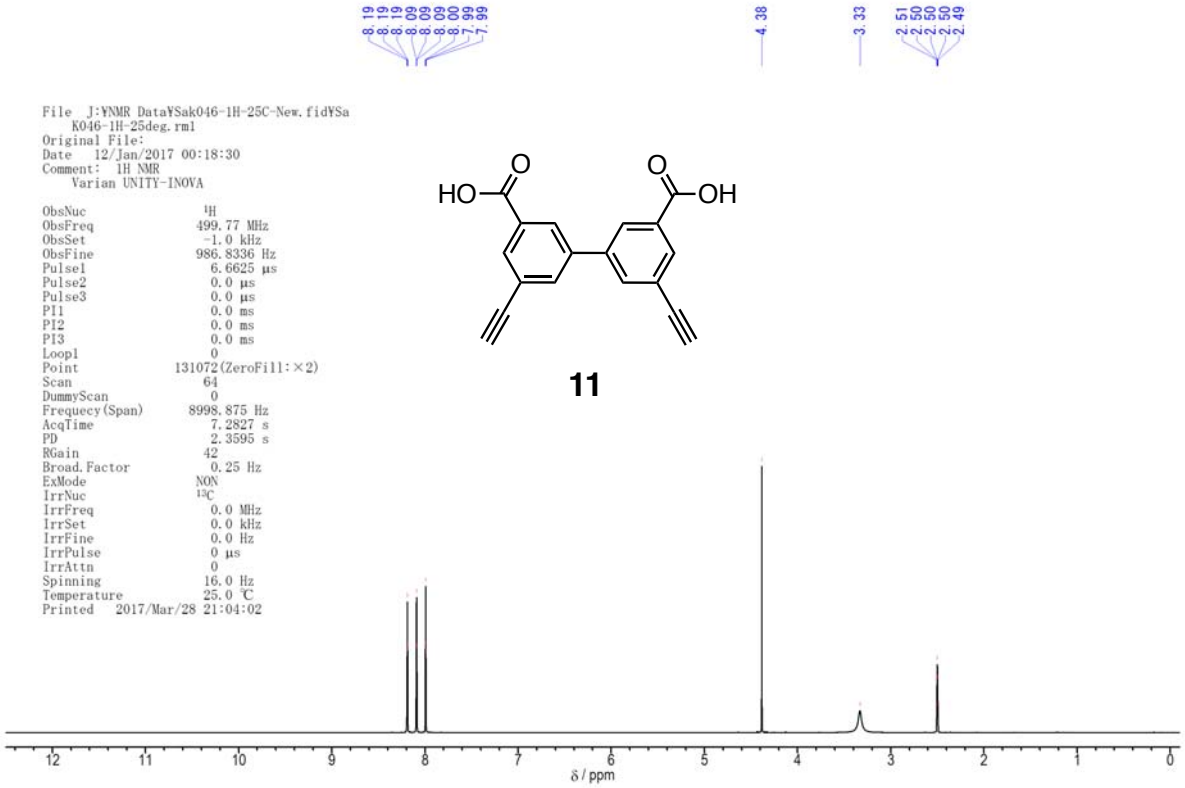

Fig. S28 ^{1}H NMR spectrum of **11** in DMSO-d_6 at 25 ℃.

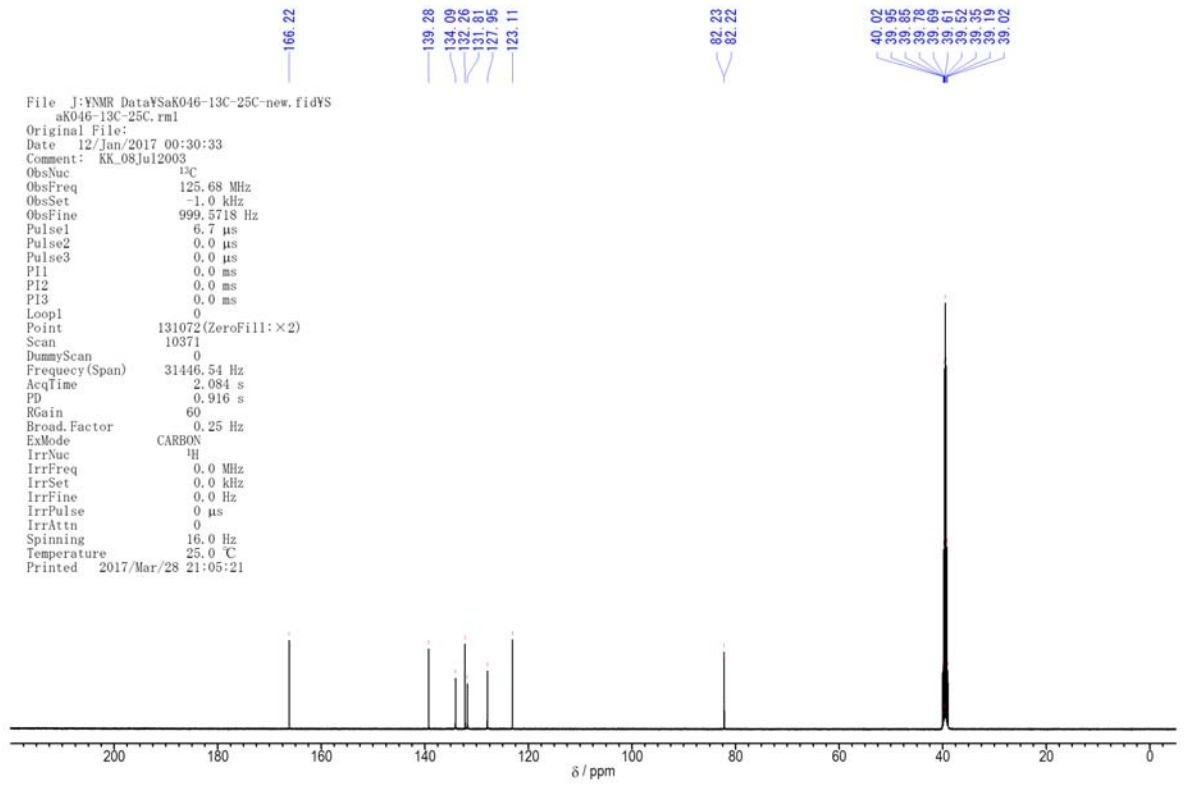

Fig. S29 ^{13}C NMR spectrum of **11** in DMSO-d_6 at 25 ℃.

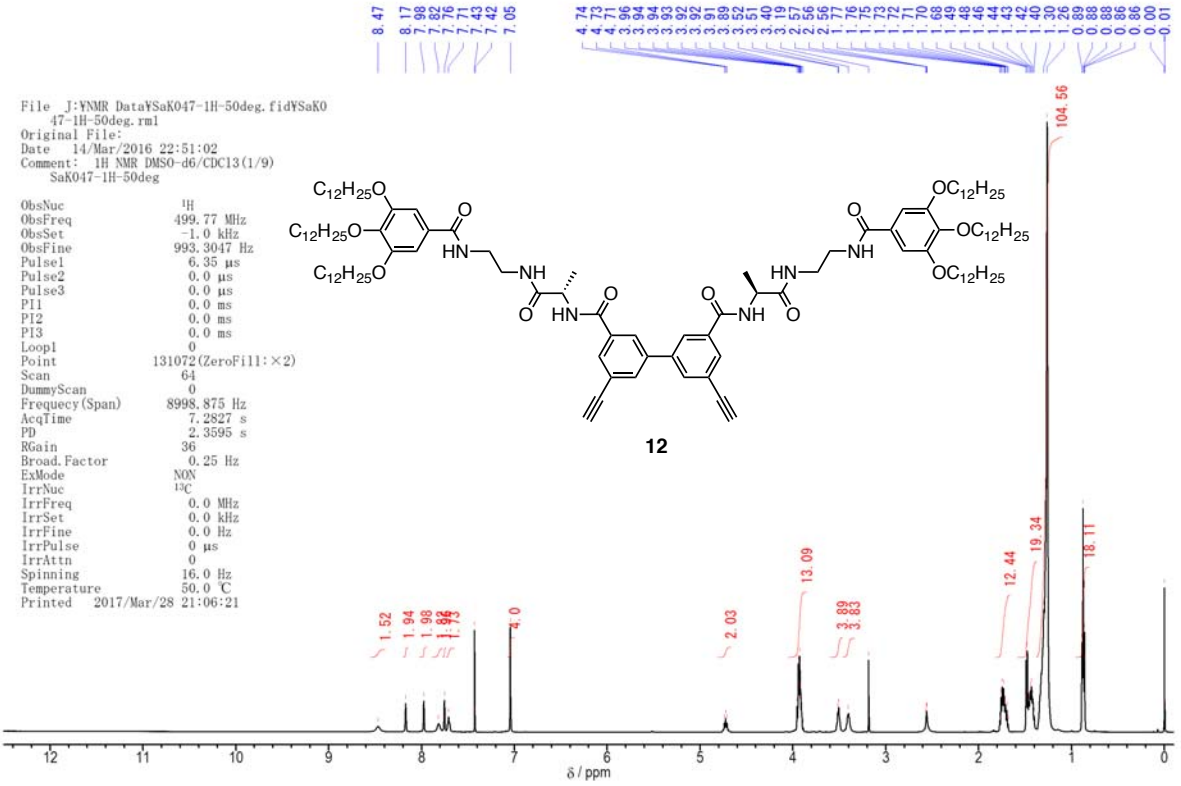

Fig. S30 ^{1}H NMR spectrum of **12** in DMSO-d_6/$CDCl_3$ = 1/9 (v/v) at 50 ºC.

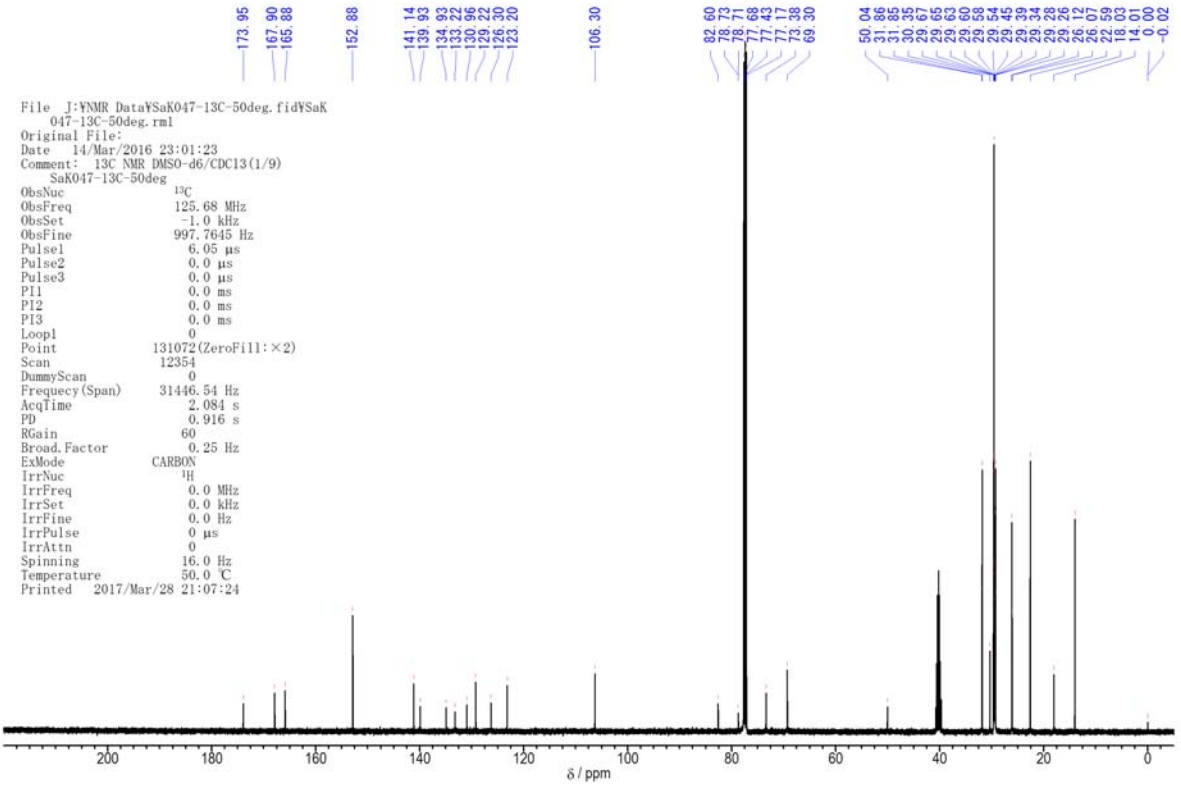

Fig. S31 ^{13}C NMR spectrum of **12** in DMSO-d_6/$CDCl_3$ = 1/9 (v/v) at 50 ºC.

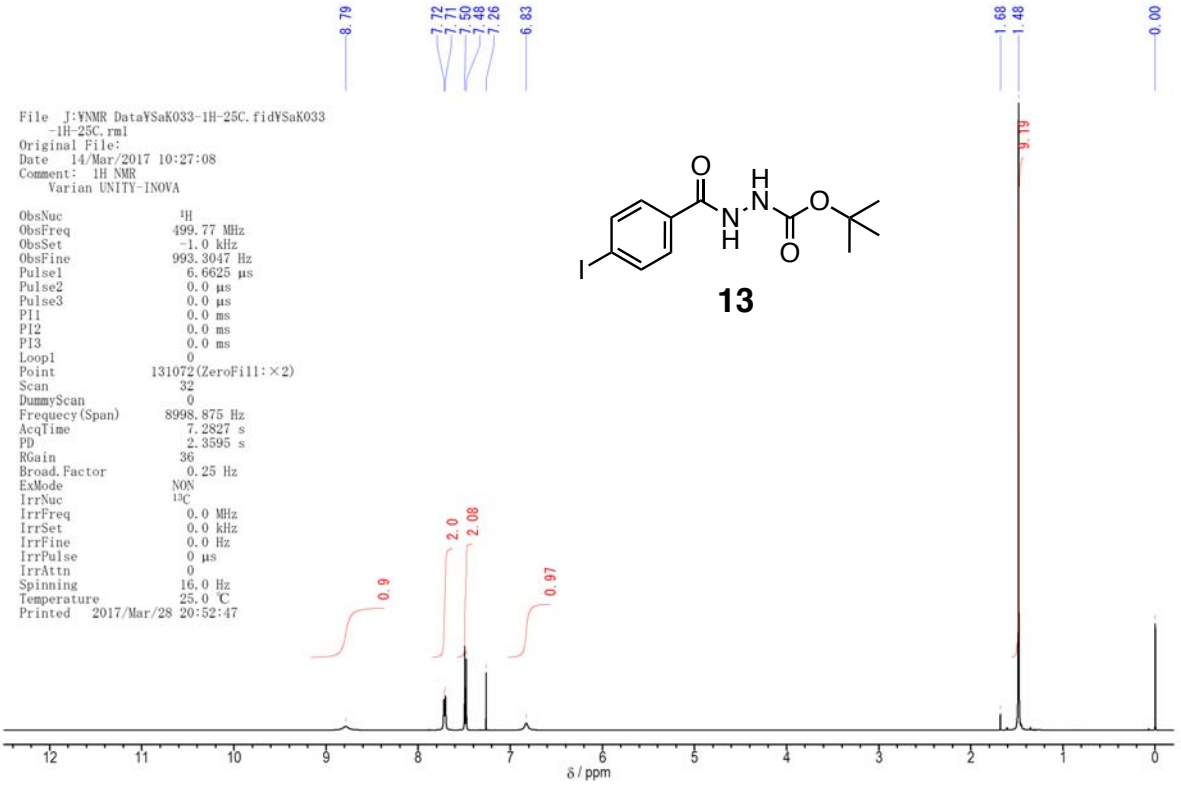

Fig. S32 ^{1}H NMR spectrum of **13** in $CDCl_3$ at 25 ºC.

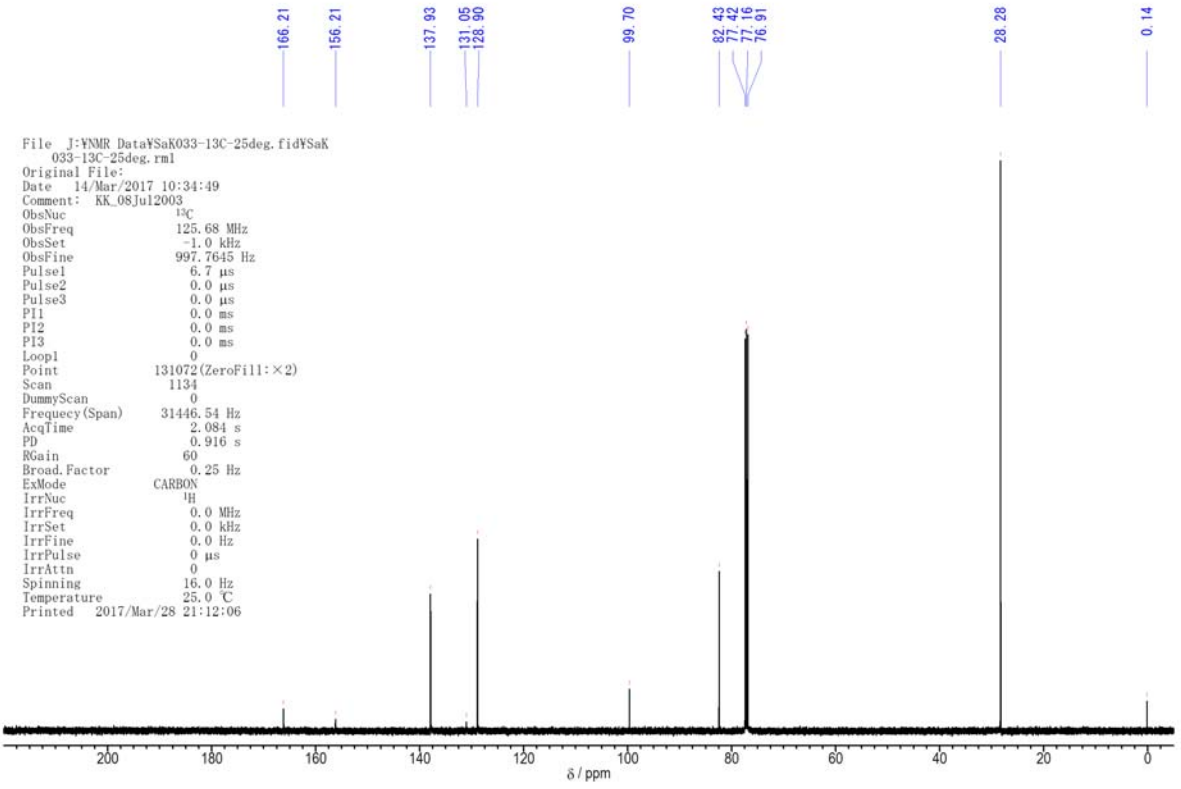

Fig. S33 ^{13}C NMR spectrum of **13** in $CDCl_3$ at 25 ºC.

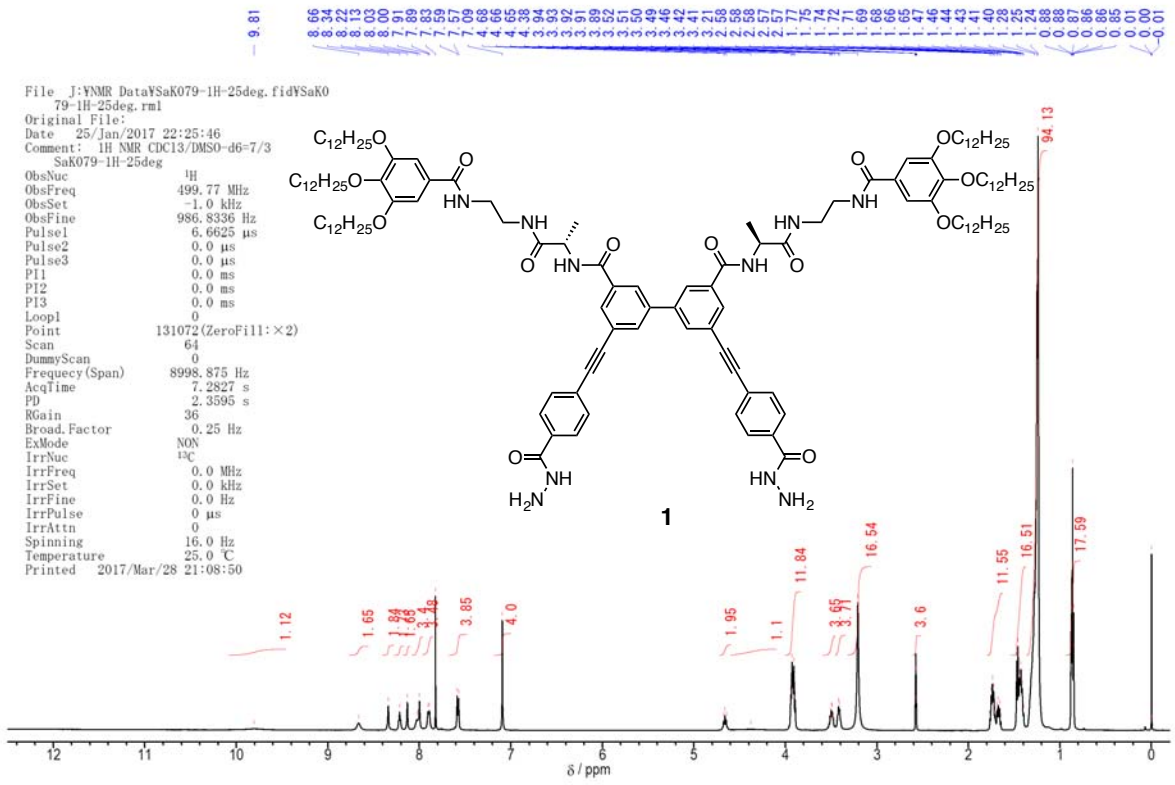

Fig. S34 ^{1}H NMR spectrum of **1** in DMSO-d_6/$CDCl_3$ = 3/7 (v/v) at 25 ºC.

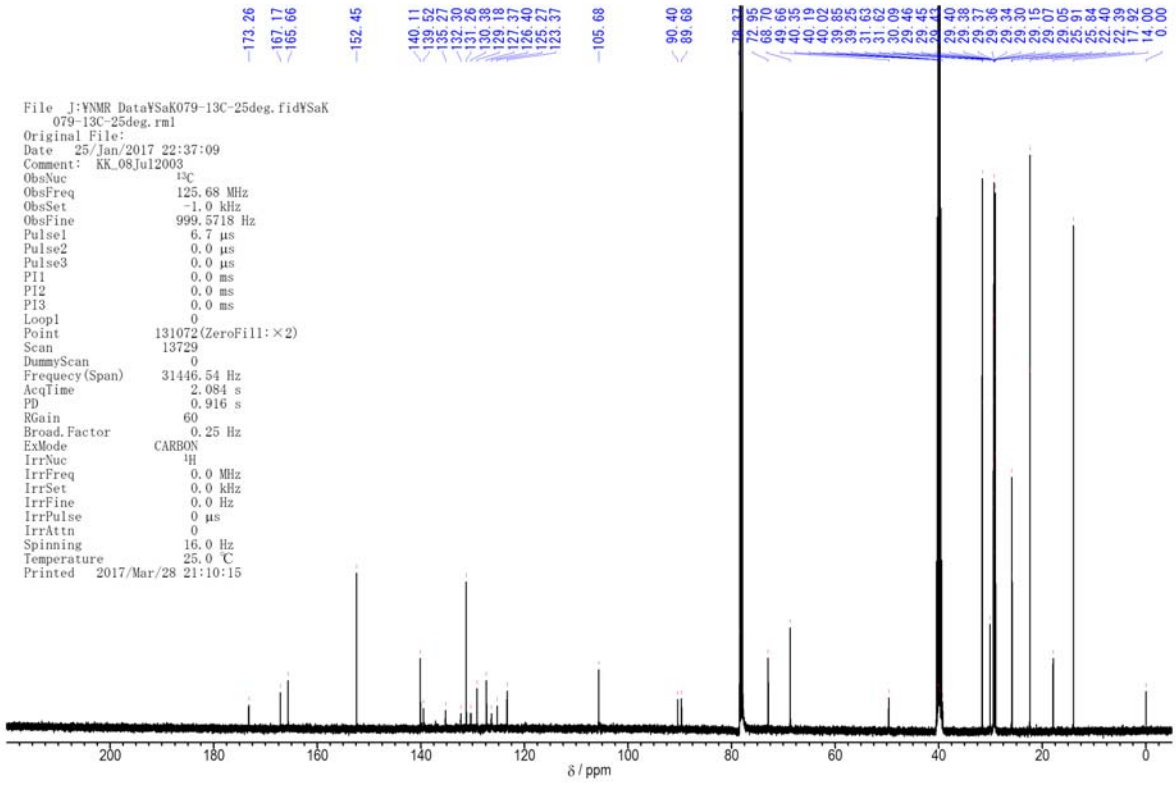

Fig. S35 ^{13}C NMR spectrum of **1** in DMSO-d_6/$CDCl_3$ = 3/7 (v/v) at 25 ºC.

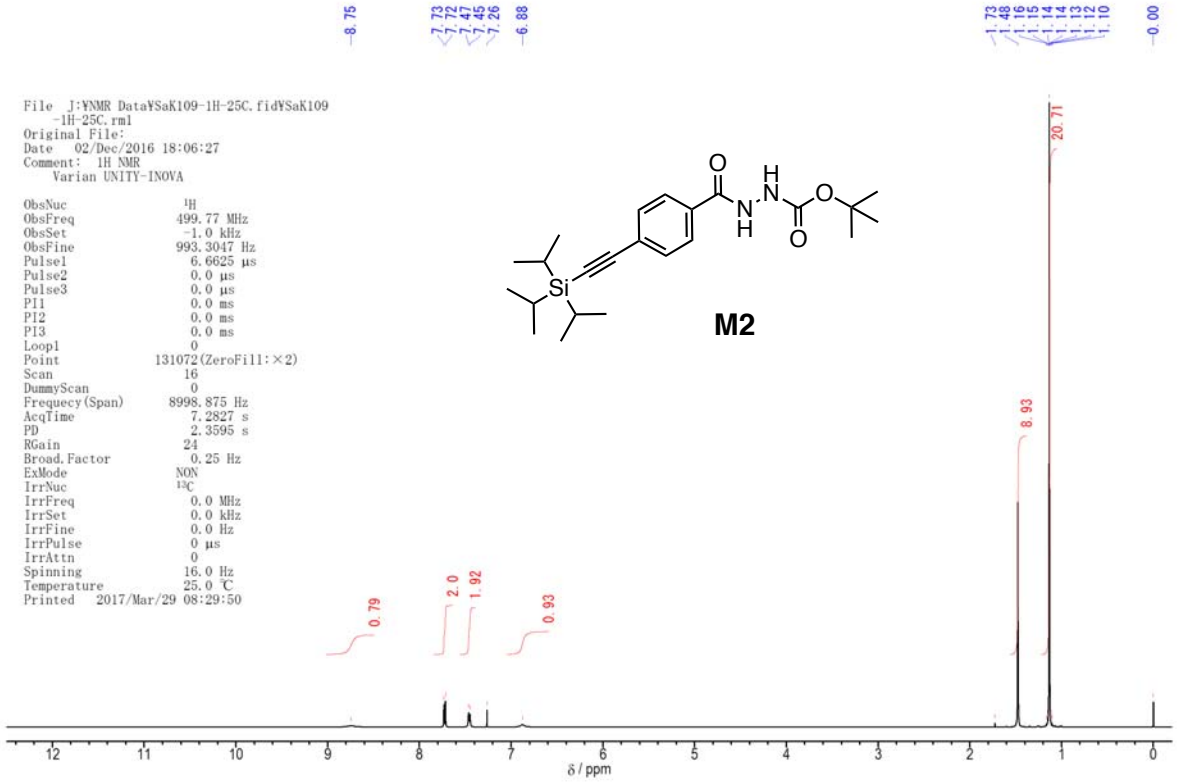

Fig. S36 ^{1}H NMR spectrum of **M2** in $CDCl_3$ at 25 ºC.

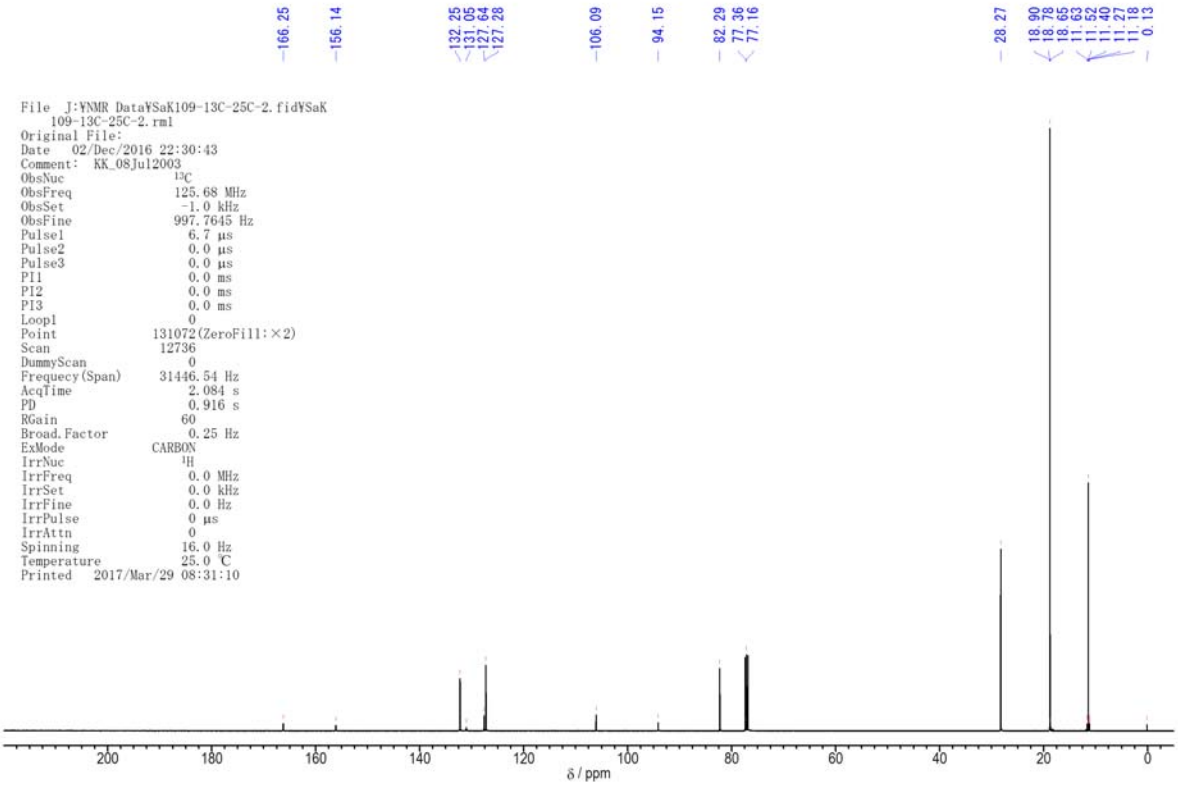

Fig. S37 ^{13}C NMR spectrum of **M2** in $CDCl_3$ at 25 ºC.

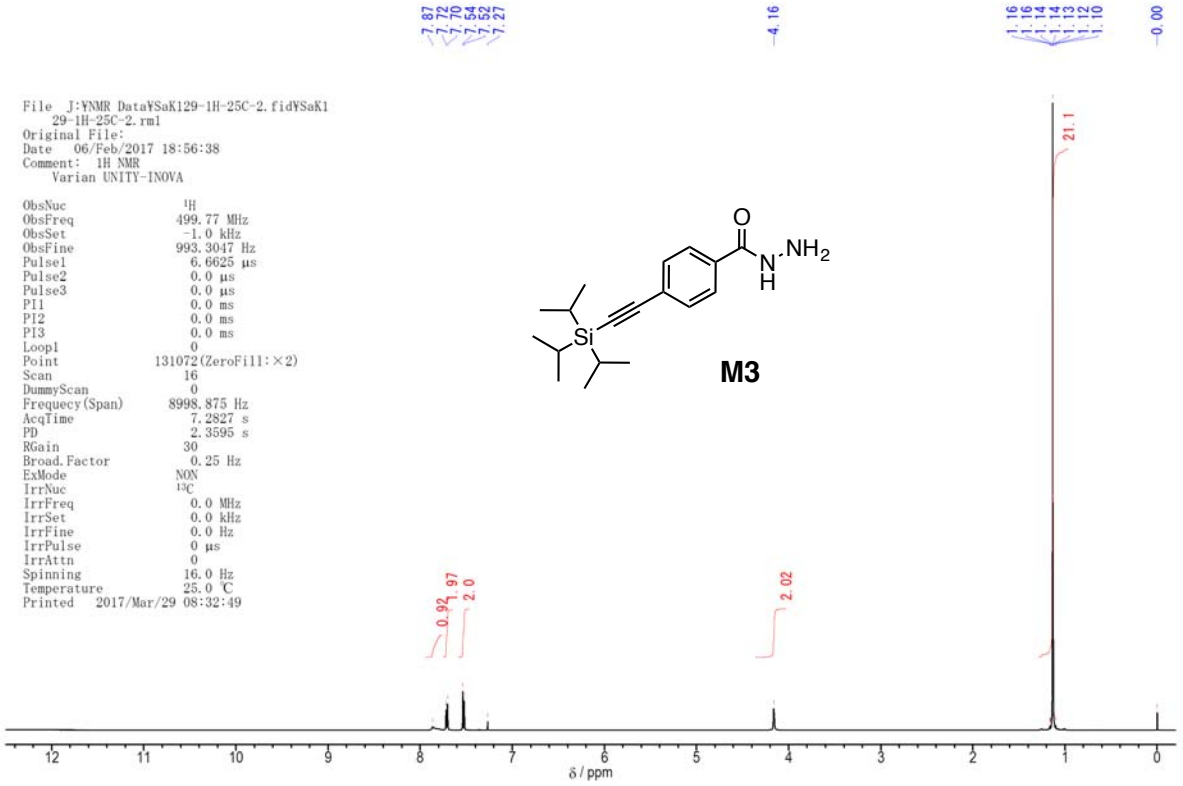

File J:¥NMR Data¥SaK129-1H-25C-2.fid¥SaK1
29-1H-25C-2.rml
Original File:
Date 06/Feb/2017 18:56:38
Comment: 1H NMR
Varian UNITY-INOVA

ObsNuc	^{1}H
ObsFreq	499.77 MHz
ObsSet	-1.0 kHz
ObsFine	993.3047 Hz
Pulse1	6.6625 μs
Pulse2	0.0 μs
Pulse3	0.0 μs
PI1	0.0 ms
PI2	0.0 ms
PI3	0.0 ms
Loop1	0
Point	131072(ZeroFill:×2)
Scan	16
DummyScan	0
Frequecy(Span)	8998.875 Hz
AcqTime	7.2827 s
PD	2.3595 s
RGain	30
Broad.Factor	0.25 Hz
ExMode	NON
IrrNuc	^{13}C
IrrFreq	0.0 MHz
IrrSet	0.0 kHz
IrrFine	0.0 Hz
IrrPulse	0 μs
IrrAttn	0
Spinning	16.0 Hz
Temperature	25.0 ℃
Printed	2017/Mar/29 08:32:49

Fig. S38 ^{1}H NMR spectrum of **M3** in $CDCl_3$ at 25 ℃.

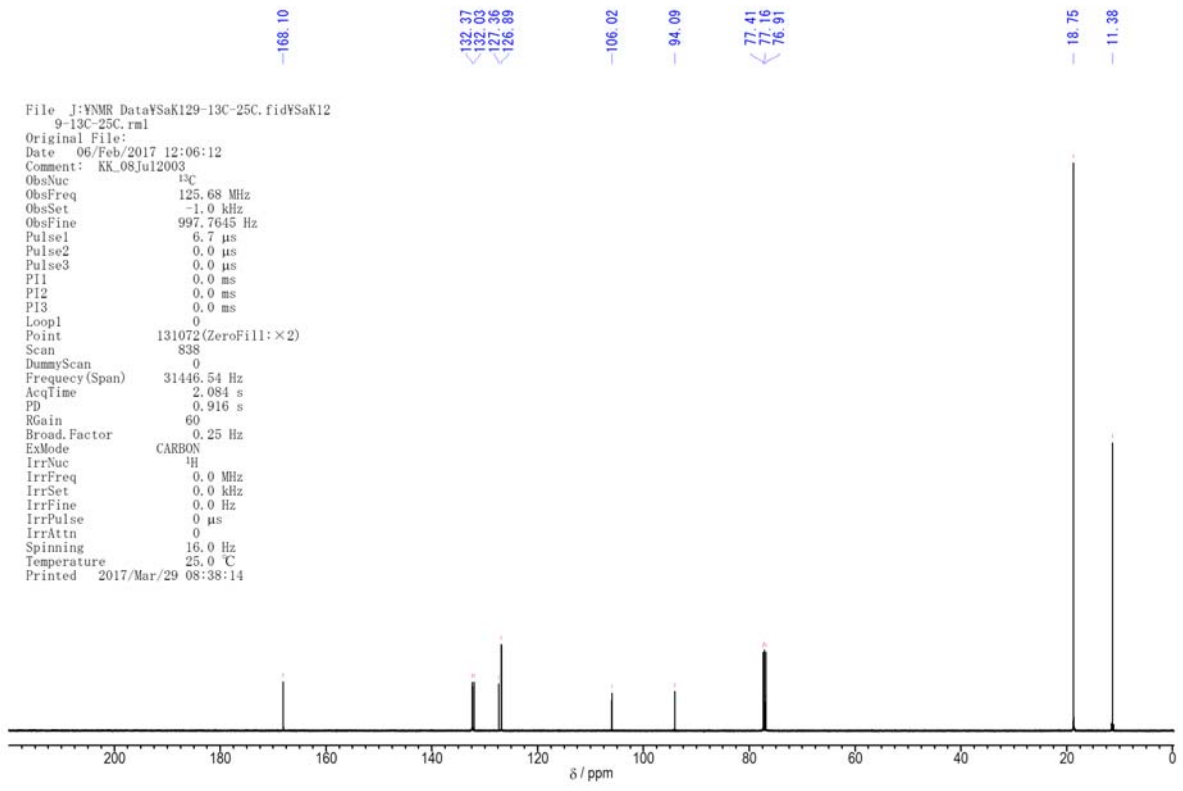

File J:¥NMR Data¥SaK129-13C-25C.fid¥SaK12
9-13C-25C.rml
Original File:
Date 06/Feb/2017 12:06:12
Comment: KK_08Jul2003

ObsNuc	^{13}C
ObsFreq	125.68 MHz
ObsSet	-1.0 kHz
ObsFine	997.7645 Hz
Pulse1	6.7 μs
Pulse2	0.0 μs
Pulse3	0.0 μs
PI1	0.0 ms
PI2	0.0 ms
PI3	0.0 ms
Loop1	0
Point	131072(ZeroFill:×2)
Scan	838
DummyScan	0
Frequecy(Span)	31446.54 Hz
AcqTime	2.084 s
PD	0.916 s
RGain	60
Broad.Factor	0.25 Hz
ExMode	CARBON
IrrNuc	^{1}H
IrrFreq	0.0 MHz
IrrSet	0.0 kHz
IrrFine	0.0 Hz
IrrPulse	0 μs
IrrAttn	0
Spinning	16.0 Hz
Temperature	25.0 ℃
Printed	2017/Mar/29 08:38:14

Fig. S39 ^{13}C NMR spectrum of **M3** in $CDCl_3$ at 25 ℃.

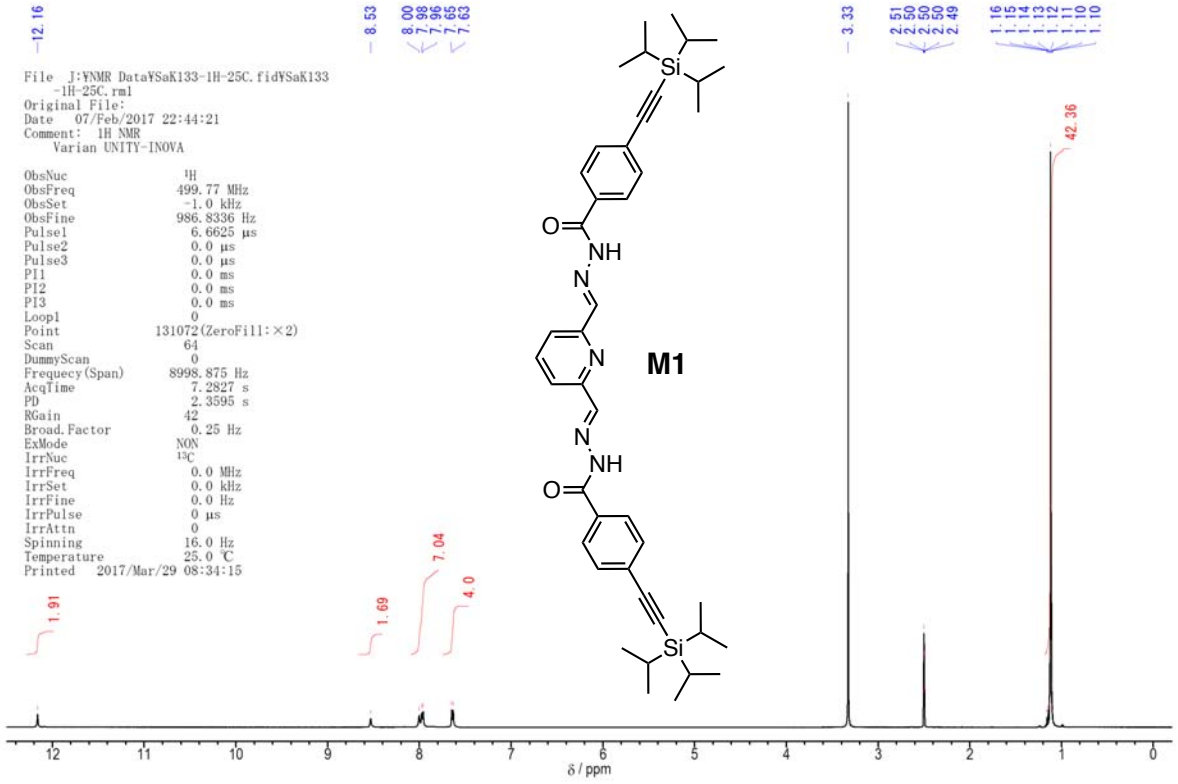

Fig. S40 ^{1}H NMR spectrum of **M1** in DMSO-d_6 at 25 ºC.

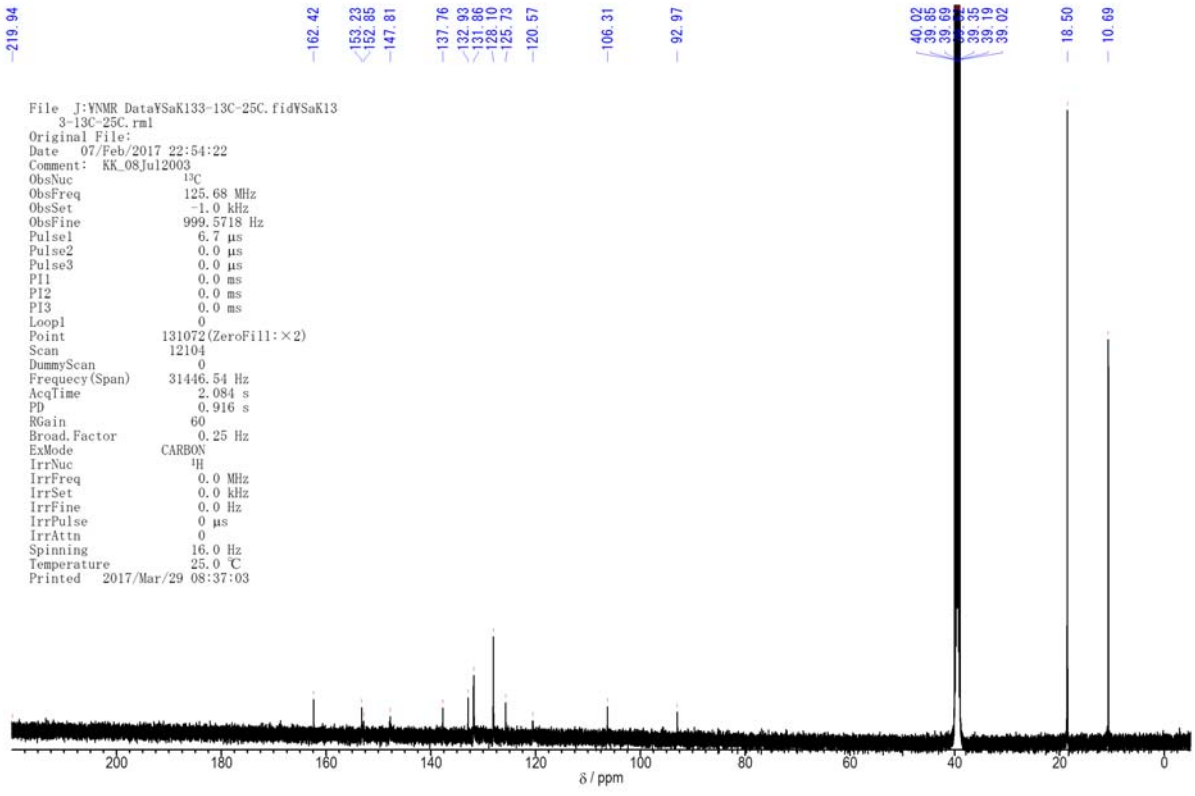

Fig. S41 ^{13}C NMR spectrum of **M1** in DMSO-d_6 at 25 ºC.